

THE GAMMA-RAY SKY

Paola Grandi, OAS-INAF



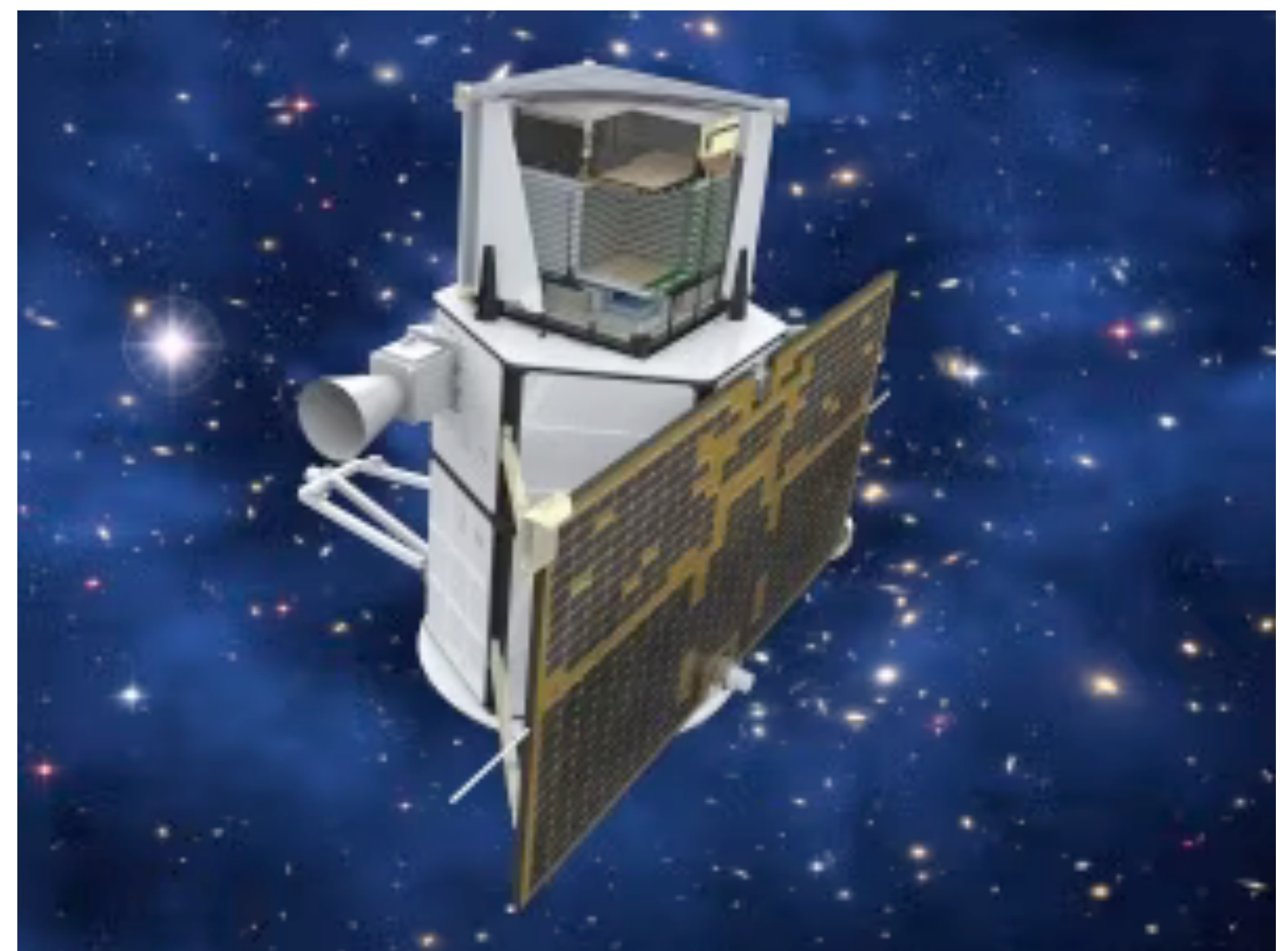
**HIGH ENERGY (HE): ~30 MeV -100 GeV
(satellites)**

**VERY HIGH ENERGY (VHE): 100 GeV -100 TeV
(satellites and Cherenkov Telescopes)**

FERMI



Agile



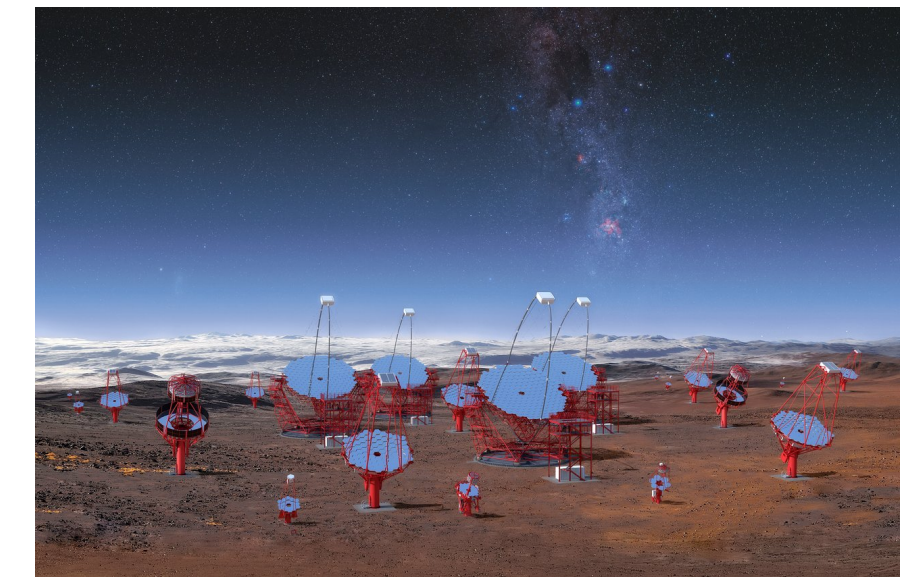
Current Cherenkov Telescopes



HESS
(southern hemisphere),

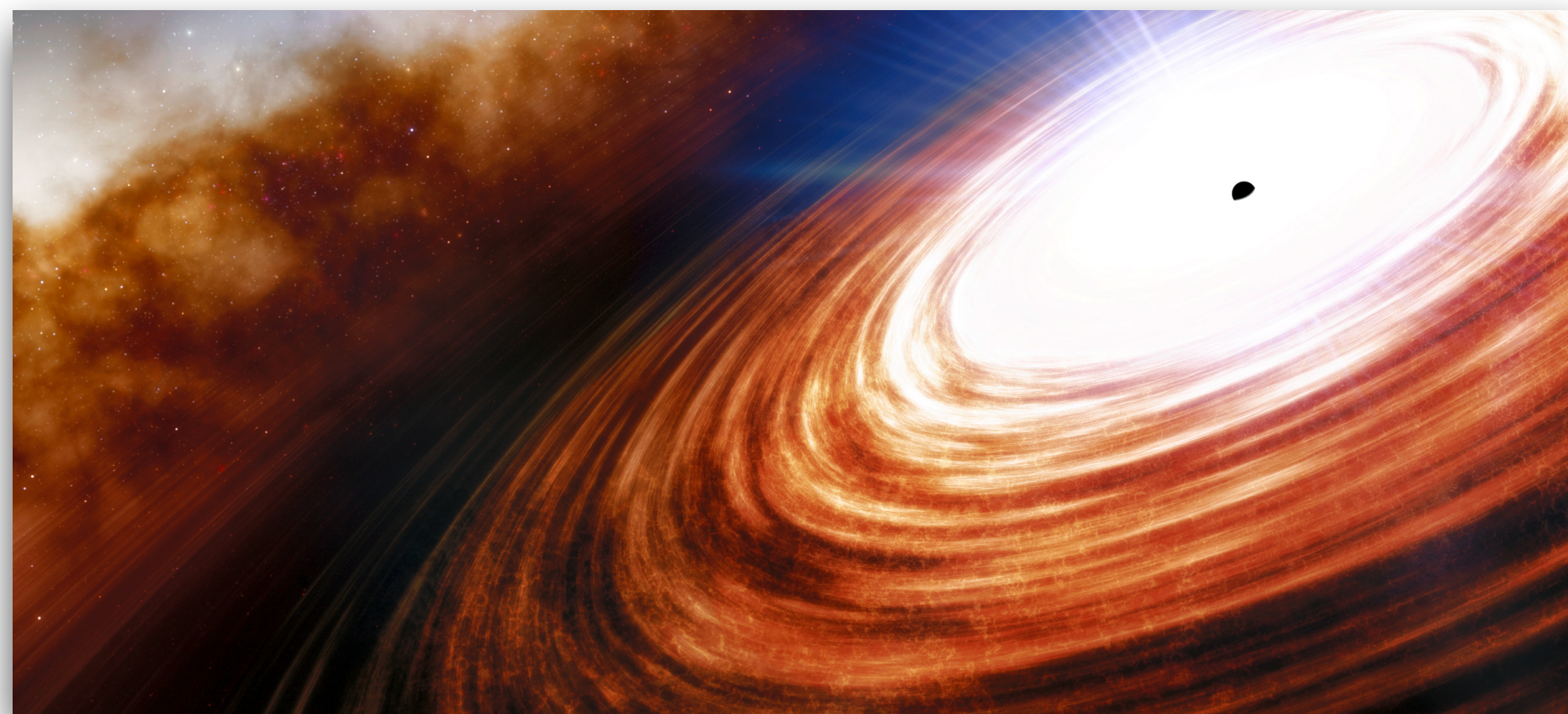
MAGIC and
VERITAS
(northern hemisphere)

CTA

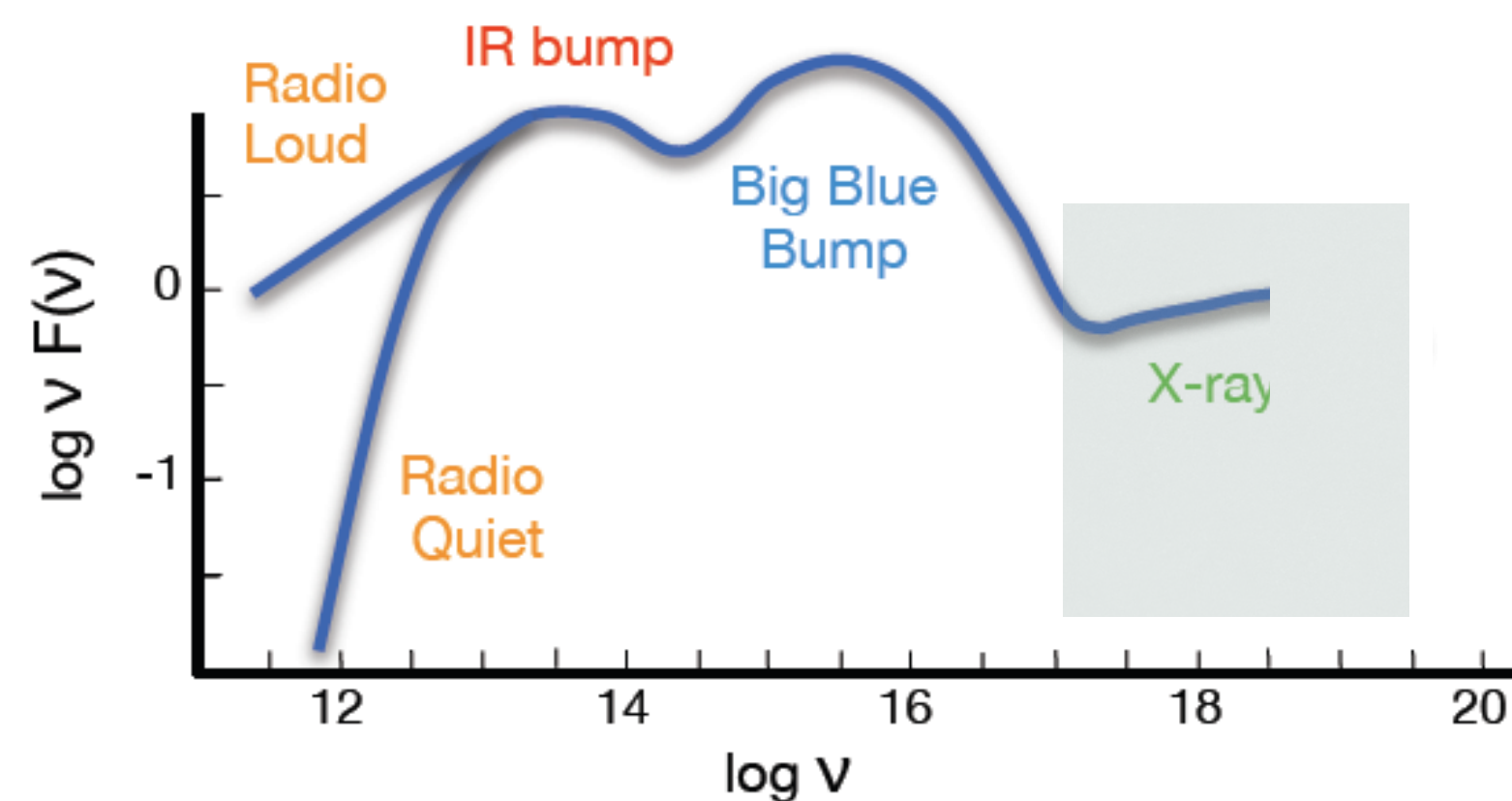


Thermal emission (Th):

Thermal radiation is dependent on the temperature T of the emitter

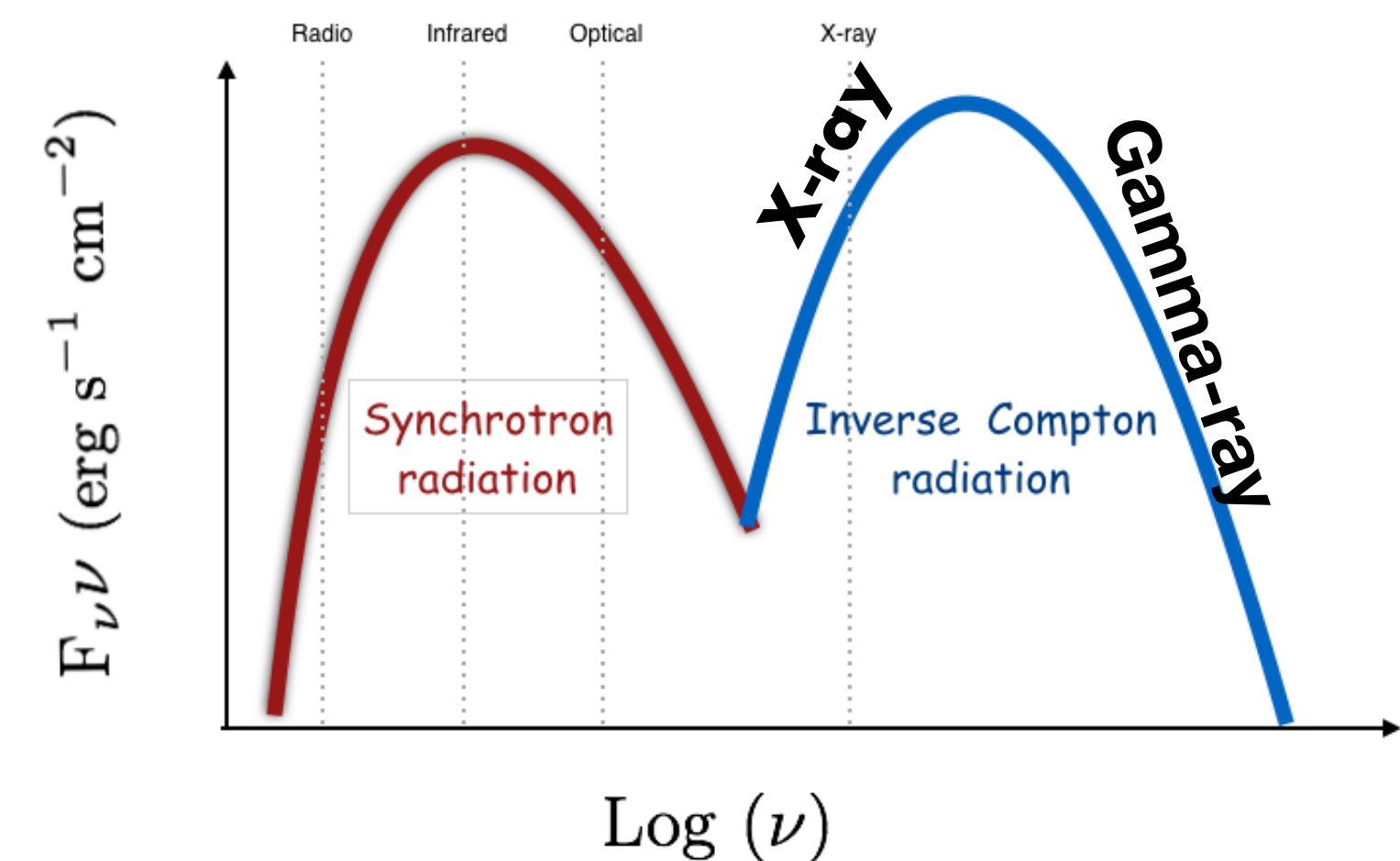
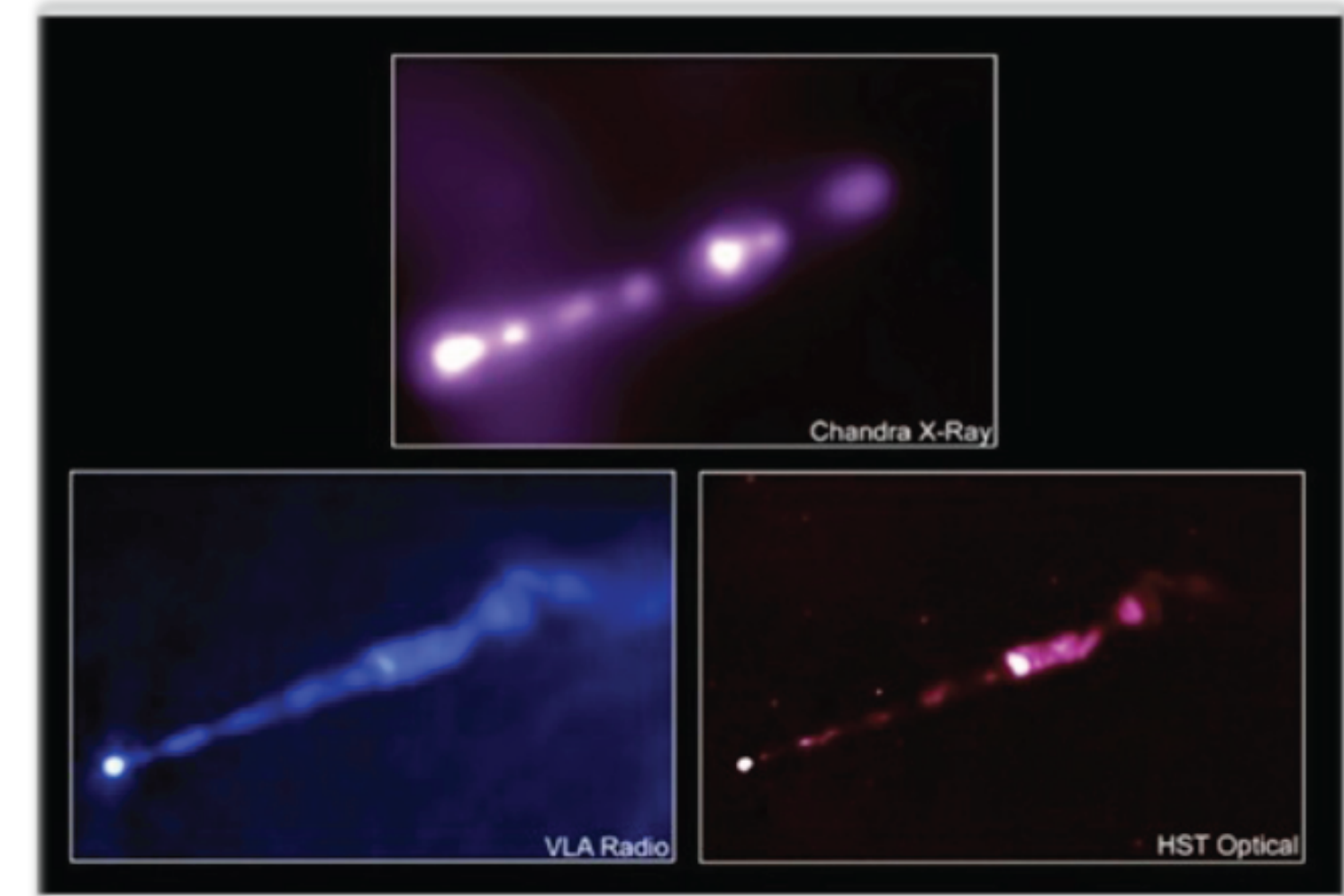


Spectral Energy Distribution (SED)



Non-Thermal emission (NTh)

Non-thermal radiation cannot be described by T and requires accelerators



Non-Thermal processes:

Given a power law distribution of electron energies

$$N(\gamma_e) = K \gamma_e^{-p}, \quad \gamma_{min} < \gamma_e < \gamma_{max}$$

Synchrotron energy density :

$$\epsilon_s(\nu) \propto K B^{\alpha+1} \nu^{-\alpha} \quad \text{erg cm}^{-3} \text{s}^{-1} \text{sr}^{-1}$$

Inverse Compton energy density :

$$\epsilon_c(\nu) \propto K \left(\int \frac{U_r(\nu_{sph}) \nu_{sph}^\alpha}{\nu_{sph}} d\nu_{sph} \right) \nu^{-\alpha}, \quad \text{erg cm}^{-3} \text{s}^{-1} \text{sr}^{-1}$$

$$p = 1 + 2\alpha,$$

B magnetic field

$U_r(\nu_{sph})$ **Specific energy density**

→ $U_r(\nu_{sph})$

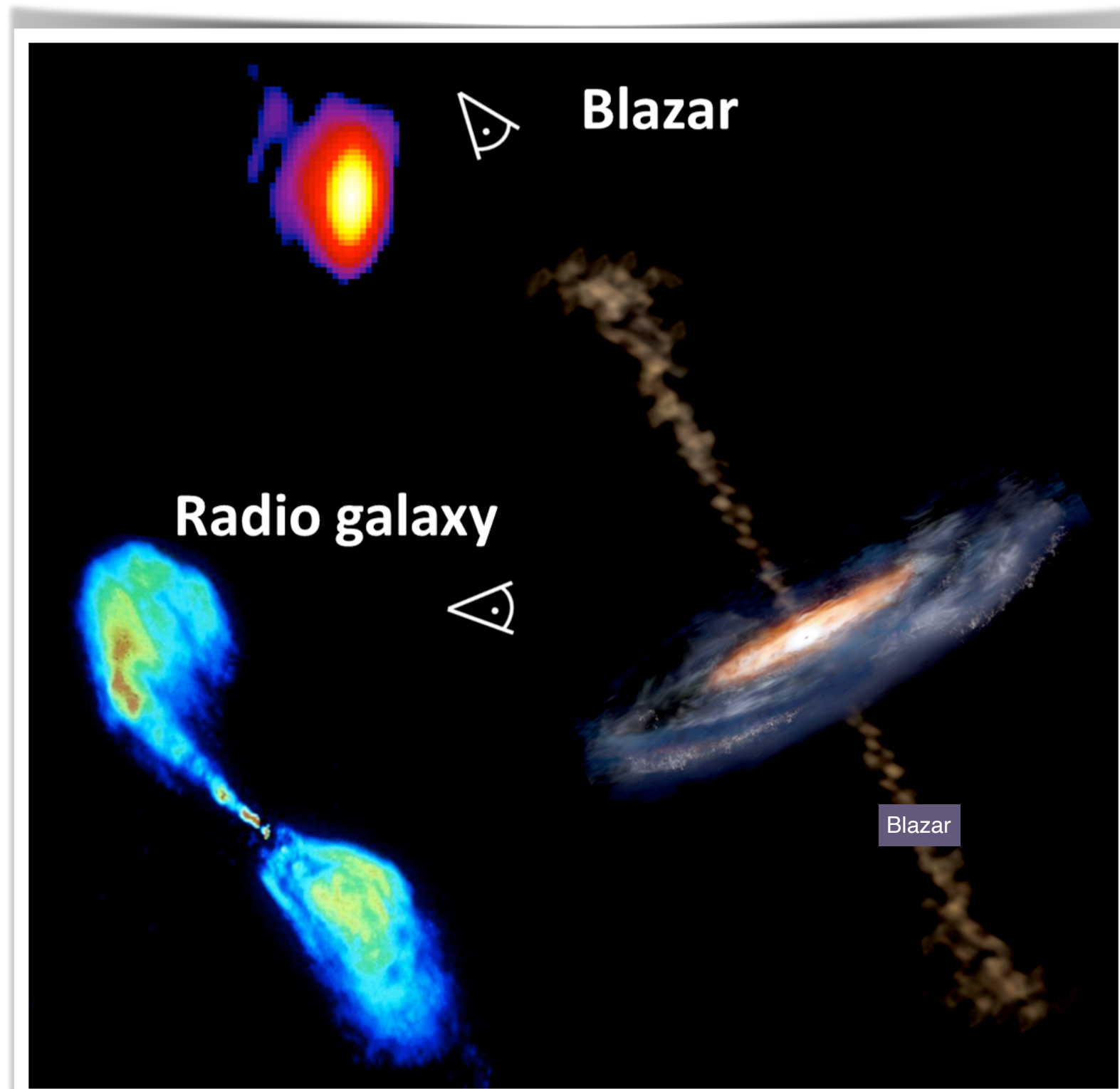
seed photons (sph)

- Synchrotron photons in the jet
- Environment photons from Accretion Flow, BLR, NLR, Torus
- Cosmic Microwave Background (CMB) photons

Non-Thermal emission:

The jet emission is strongly **Doppler boosted**

The key parameter is the **Doppler Factor $\delta(\beta, \theta)$**



$$\delta = [\gamma(1 - \beta \cos \theta)]^{-1}$$

$= \sqrt{1 - \beta^2}$
Lorentz factor

$= v/c$
bulk velocity

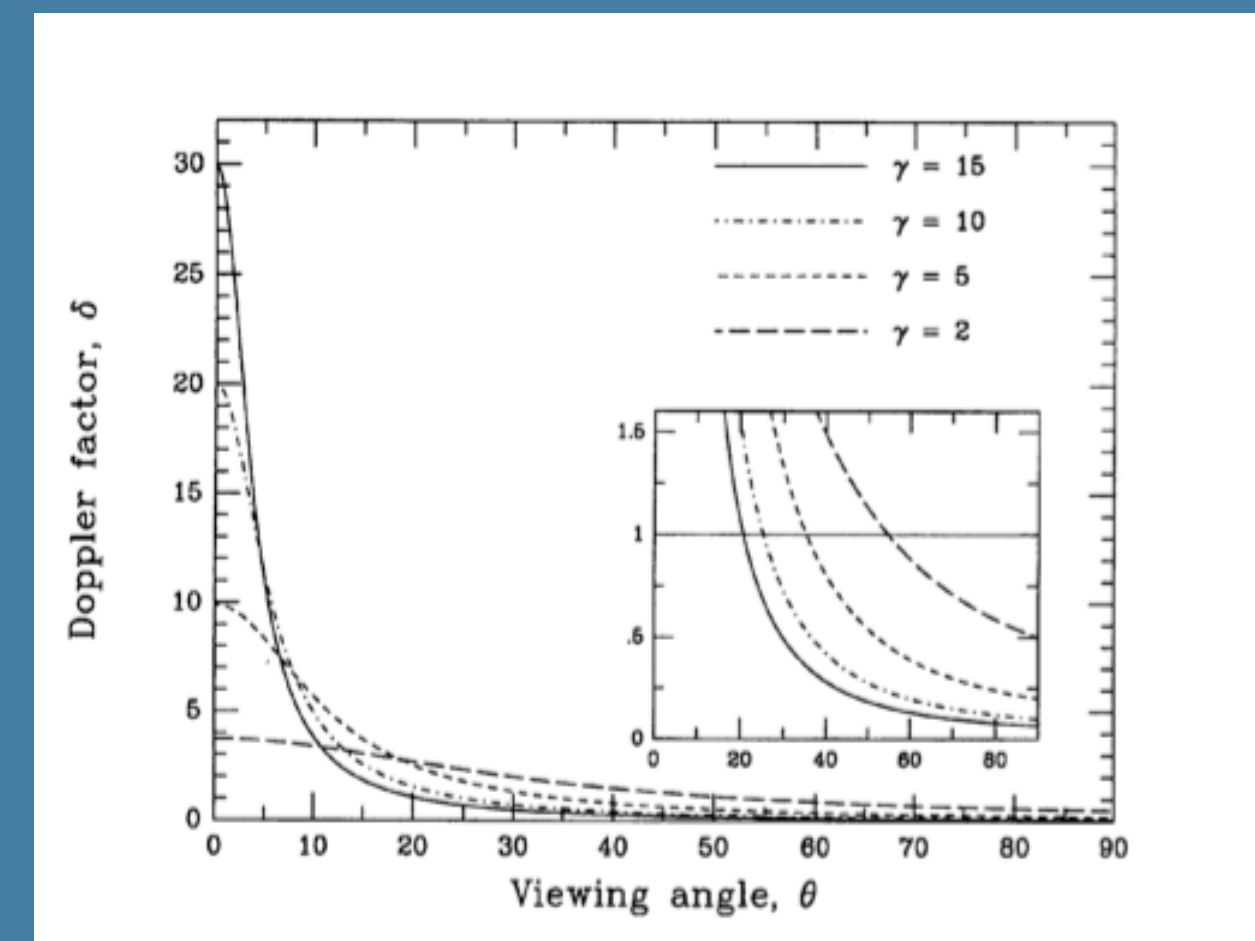
angle between
the jet axis and
the line of sight

For an **intrinsic** power law spectrum:

$$F'(v') = K (v')^{-\alpha}$$

the **observed** flux density is

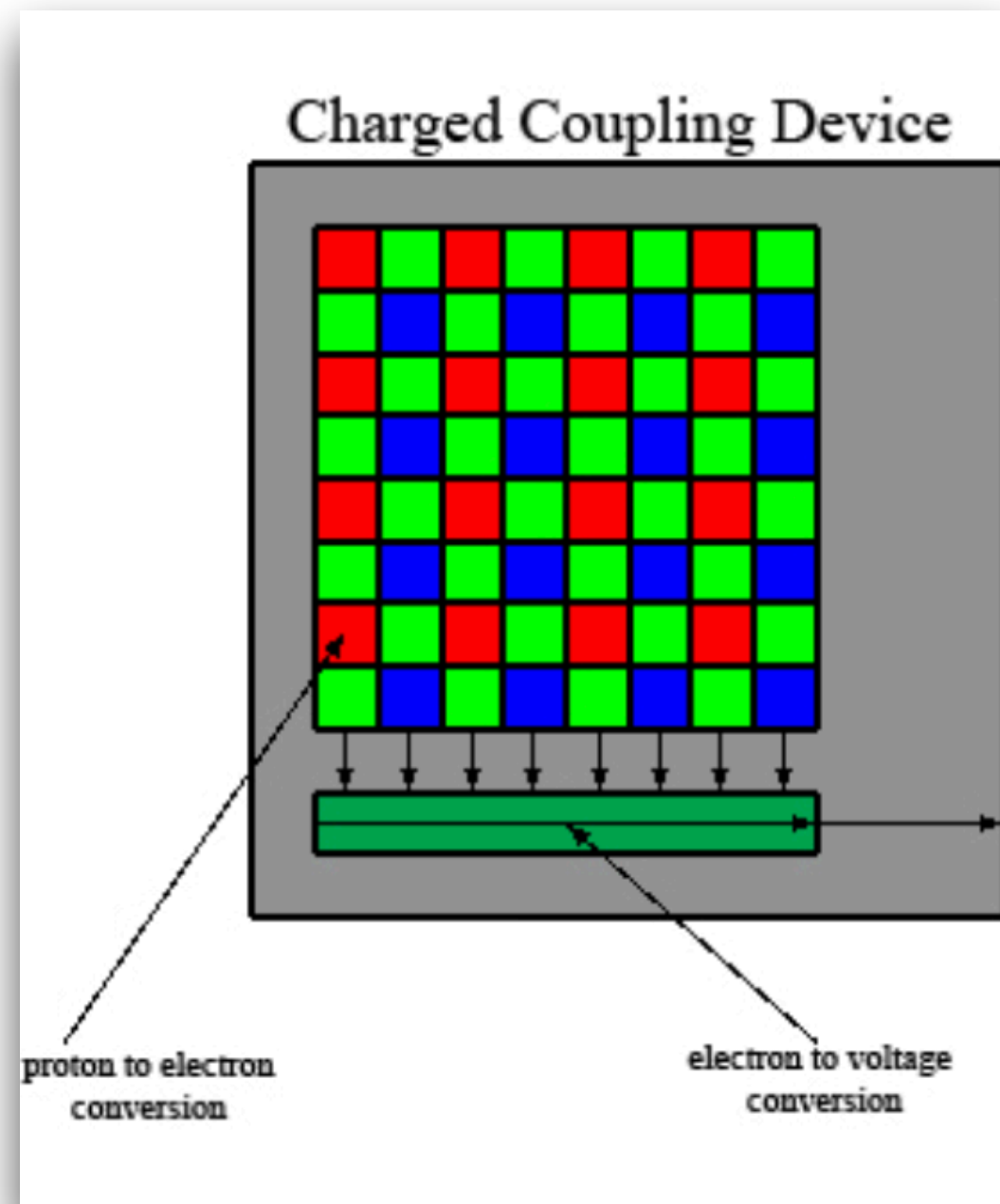
$$F_v(v) = \delta^{3+\alpha} F'_{v'}(v)$$



Detectors

X-rays

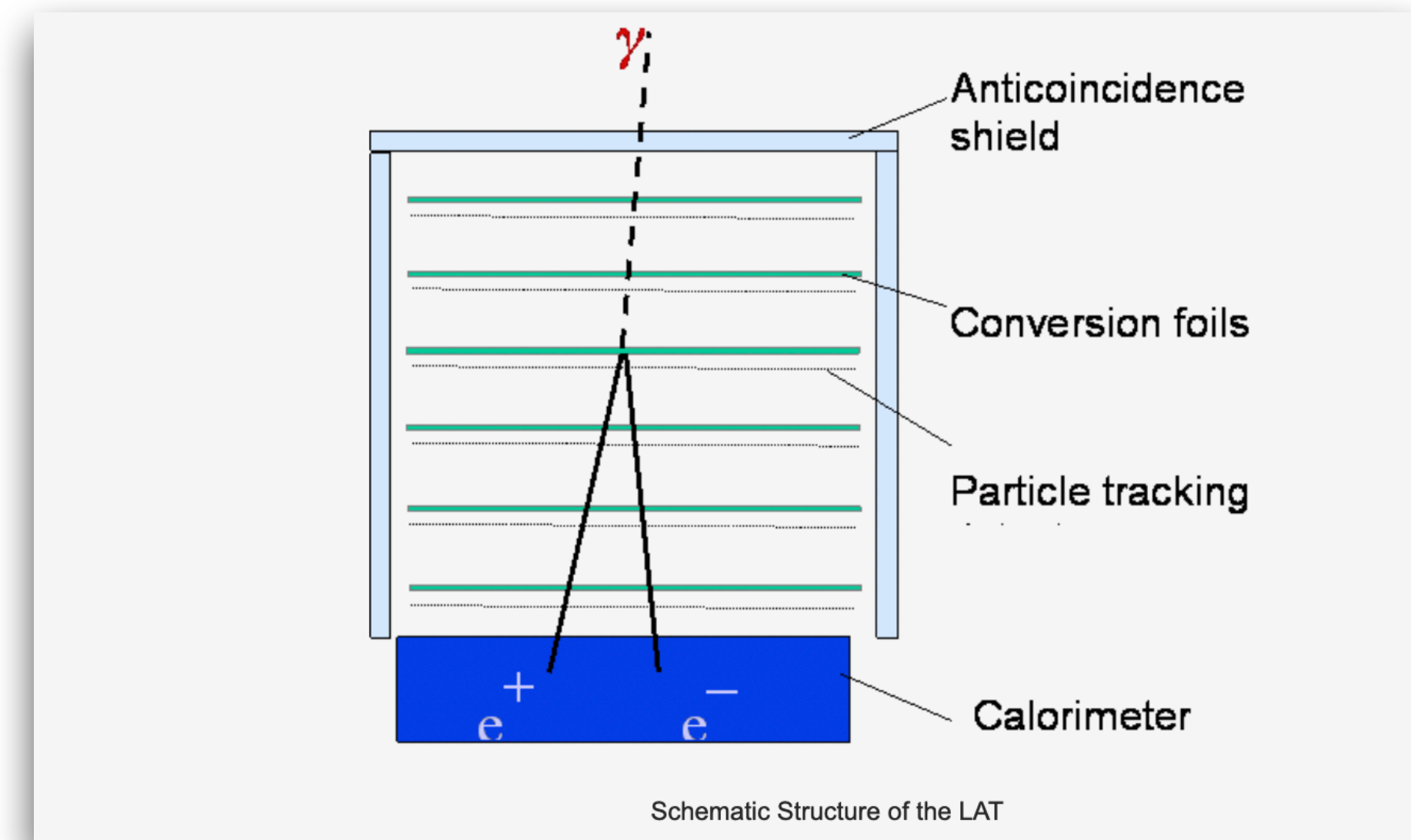
The photoelectric effect lies at the heart of CCD operation



- Photons interact in a semiconductor substrate (usually silicon) and are converted into electron-hole pairs
- Applied electric field used to collect charge carriers (usually electrons) and store them in pixels
- Pixels are "coupled" and can transfer their stored charge to neighboring pixels
- Stored charge is transferred to a readout amplifier
- At readout amplifier, charge is sensed and digitized (SEE DADINA LESSON)

Gamma-rays

HE Photons interact with matter by electron-positron pair production ($\gamma \rightarrow e^- + e^+$)



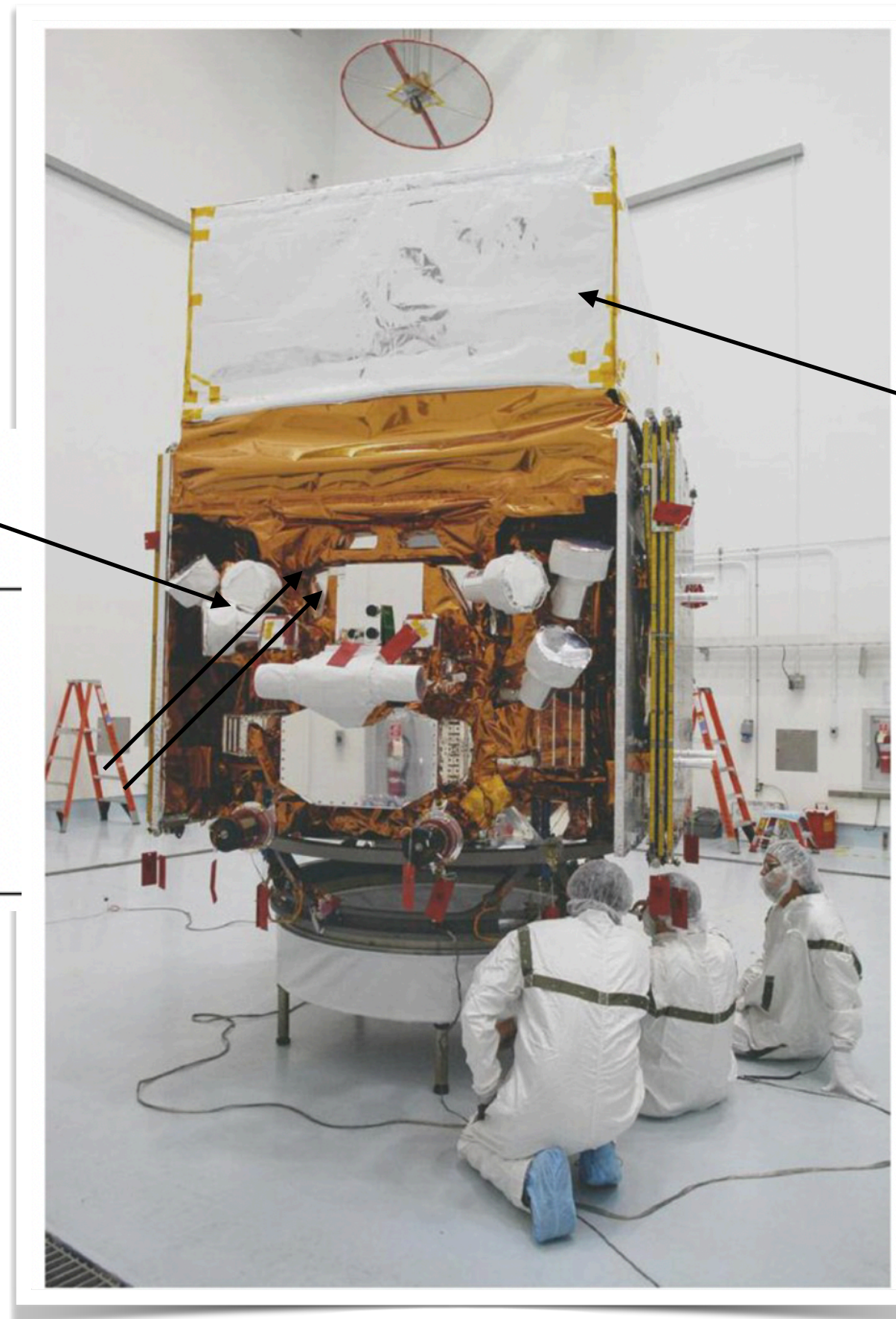
FERMI Satellite: Scientific Instruments

FERMI: Sky Survey Observing Mode with a full sky coverage every 2 orbits (3hours)

Gamma-ray Burst Monitor

Table 1 Key Characteristics of the *Fermi* Gamma-ray Burst Monitor

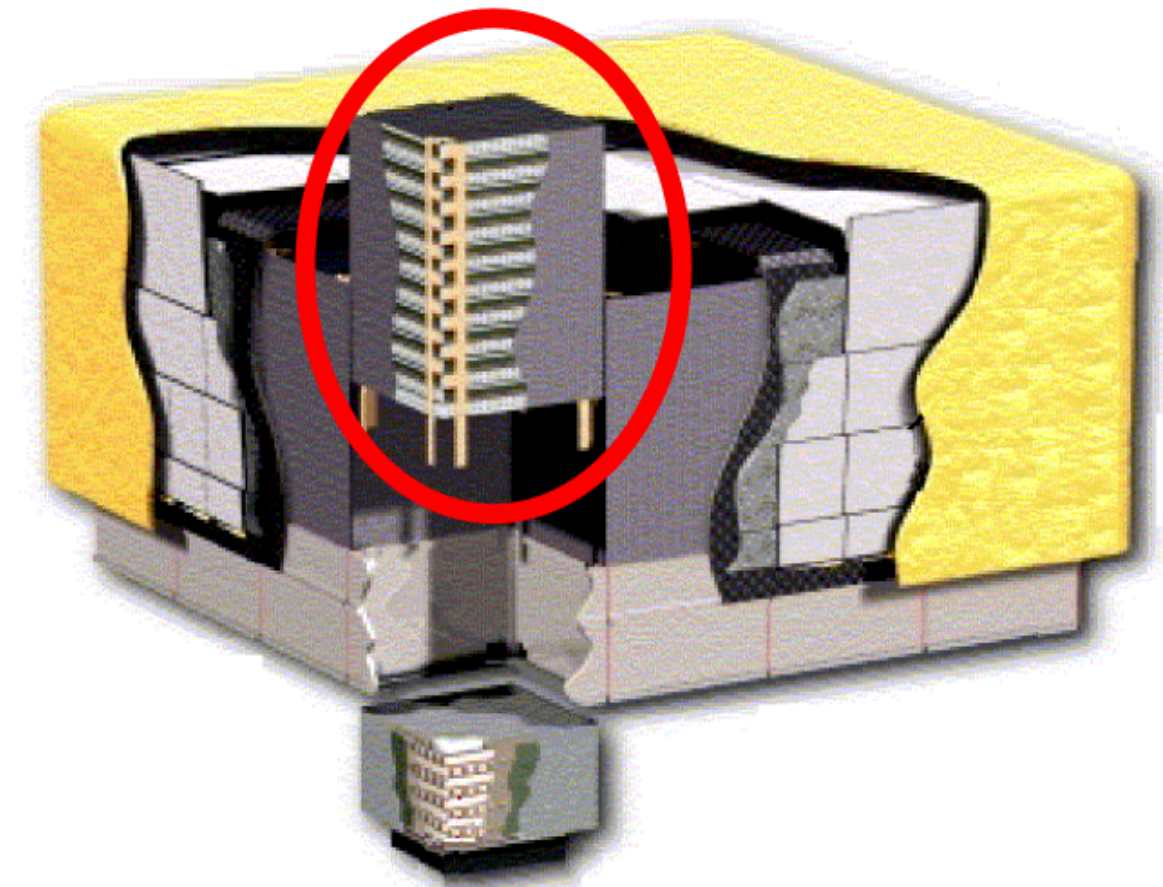
Property	Value
Energy Range	8 keV – 1 MeV (NaI) 200 keV – 40 MeV (BGO)
Energy Resolution	<12% FWHM at 511 keV
Effective field of view	> 8 steradians (excluding Earth occultation)
Timing accuracy	< 2 μ sec absolute
Timing resolution	2 μ sec



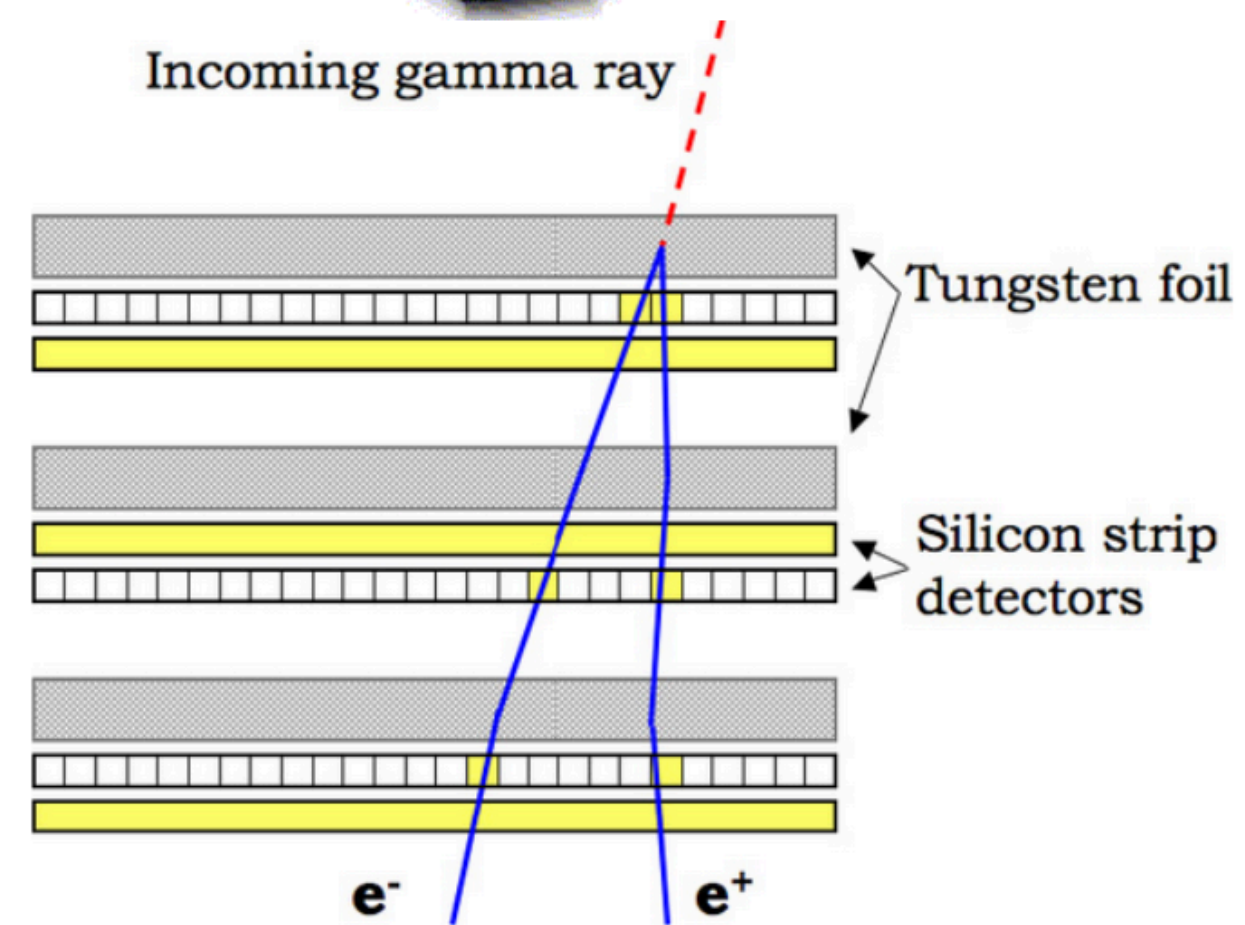
Large Area Telescope

Note: Chandra, XMM-NEWTON, NuStar : point single sources

Large Area Telescope



The LAT detects γ -rays in the energy range from 20 MeV to more than 1 TeV, measuring their arrival times, energies, and directions. The field of view of the LAT is ~ 2.7 sr at 1 GeV and above.



Picture of a tracker plane:

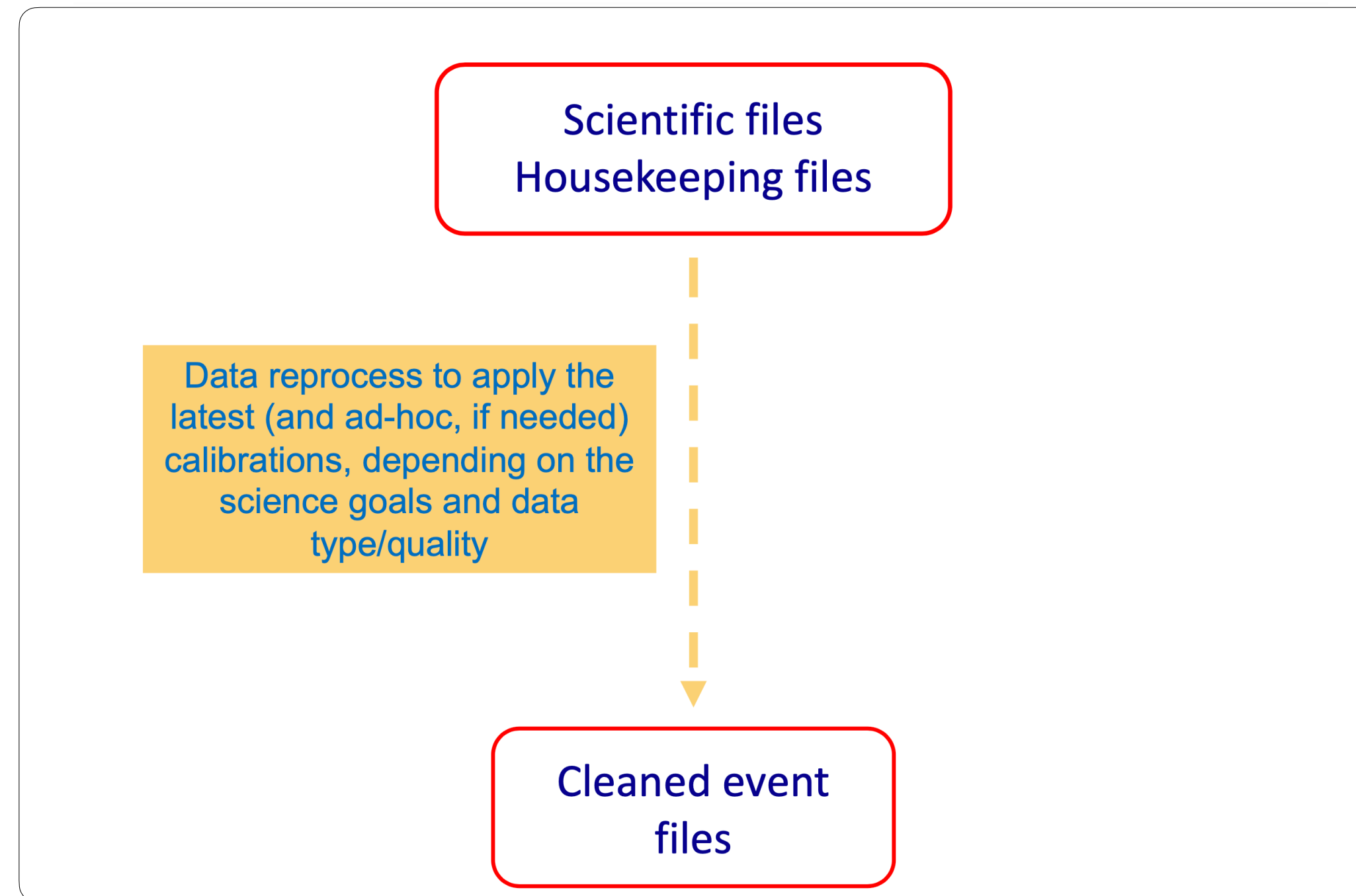
The LAT consists of an array of 16 tracker (TKR) modules, 16 calorimeter (CAL) modules, and a segmented ACD.

The tracking section of the LAT has 36 layers of silicon strip detectors interleaved with 16 layers of tungsten foil (12 thin layers, 0.03 radiation length, at the top or *Front* of the instrument, followed by four thick layers, 0.18 radiation lengths, in the *Back* section). The silicon strips track charged particles, and the tungsten foils facilitate conversion of γ -rays to positron-electron pairs. Beneath the tracker is a calorimeter.

The information from the anticoincidence detector, tracker and calorimeter is combined to estimate the energy and direction of the gamma ray.

X-ray and Gamma-ray data reductions: similar procedure

Data reduction



IMAGE

SPECTRUM

LIGHT CURVE

More details, later, on the Gamma-ray data reduction (Tutorial of Ettore Bronzini)

X-rays

Scientific files
Housekeeping files

Cleaned event
files

Gamma-rays : FERMI

Scientific file -> photon file
includes the energy of the event, the position, and information about the quality of the event reconstruction.

Housekeeping file-> spacecraft file
contains spacecraft position and orientation information for 30 second intervals.

Cleaned file that is the starting point for the production of images, spectra and light curves

FERMI LAT events are classified on their photon probability and the quality of their reconstruction.

Standard Hierarchy for LAT Event Classes				
Event Class	evclass	Photon File	Extended File	Description
P8R3_TRANSIENT020	16		X	Transient event class with background rate equal to two times the A10 IGRB reference spectrum.
P8R3_TRANSIENT010	64		X	Transient event class with background rate equal to one times the A10 IGRB reference spectrum.
P8R3_SOURCE	128	X	X	This event class has a residual background rate that is comparable to P7REP_SOURCE. This is the recommended class for most analyses and provides good sensitivity for analysis of point sources and moderately extended sources.
P8R3_CLEAN	256	X	X	This class is identical to SOURCE below 3 GeV. Above 3 GeV it has a 1.3-2 times lower background rate than SOURCE and is slightly more sensitive to hard spectrum sources at high galactic latitudes.
P8R3_ULTRACLEAN	512	X	X	This class has a background rate very similar to ULTRACLEANVETO.
P8R3_ULTRACLEANVETO	1024	X	X	This is the cleanest Pass 8 event class. Its background rate is 15-20% lower than the background rate of SOURCE class below 10 GeV, and 50% lower at 200 GeV. This class is recommended to check for CR-induced systematics as well as for studies of diffuse emission that require low levels of CR contamination.
P8R3_SOURCEVETO	2048	X	X	This class has the same background rate than the SOURCE class background rate up to 10 GeV but, above 50 GeV, its background rate is the same as the ULTRACLEANVETO one while having 15% more acceptance.

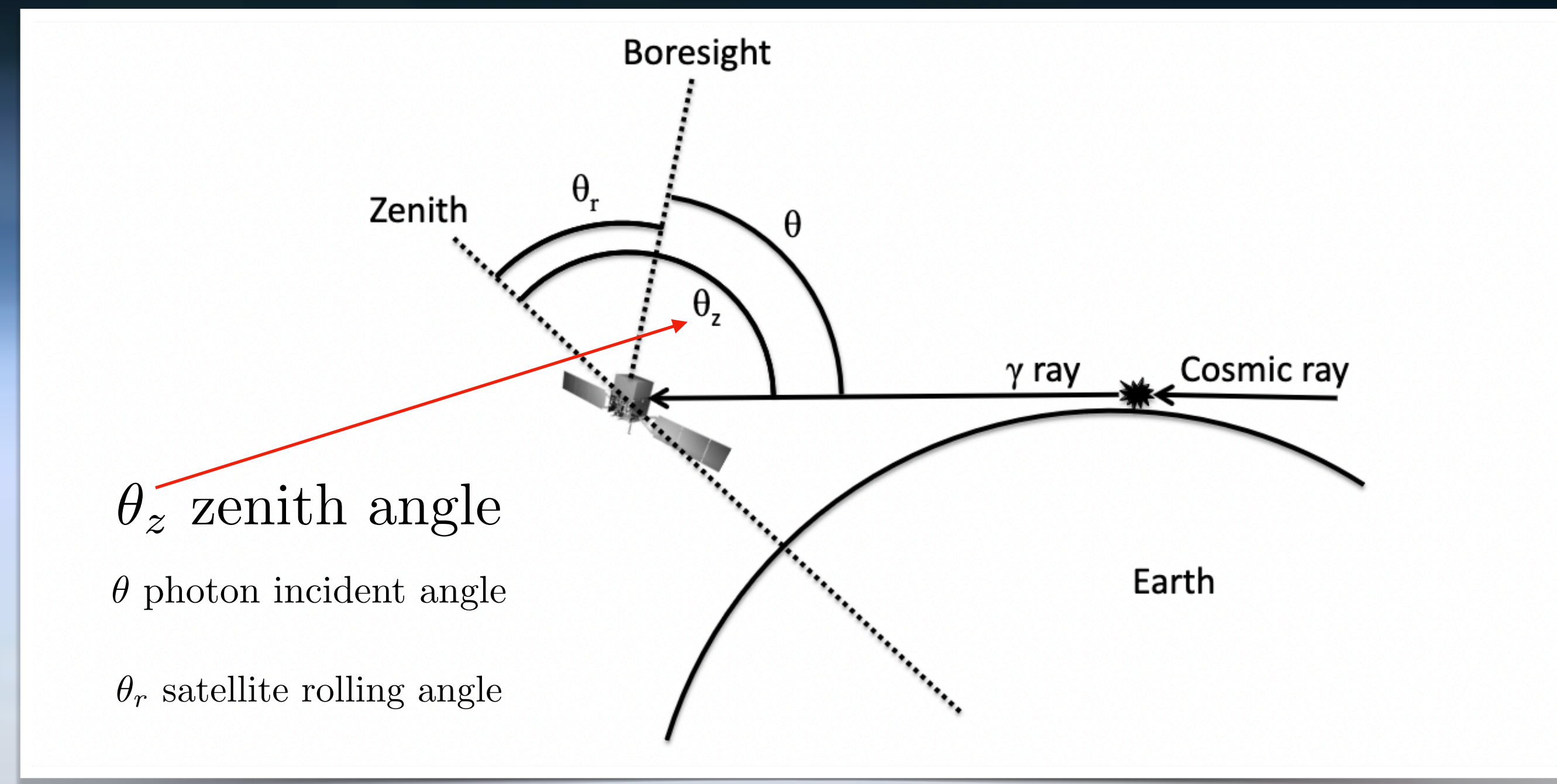
Each event class was partitioned in two conversion event types (front and back), depending on the location of the Tracker layer where the photon-to-pair conversion occurred. Photons that convert in the front section have intrinsically better angular resolution than those that convert in the back section.

Conversion Type Partition		
Event Type	evtype	Description
FRONT	1	Events converting in the Front-section of the Tracker. Equivalent to convtype=0.
BACK	2	Events converting in the Back-section of the Tracker. Equivalent to convtype=1.

Important selection to reduce the background: zenith angle

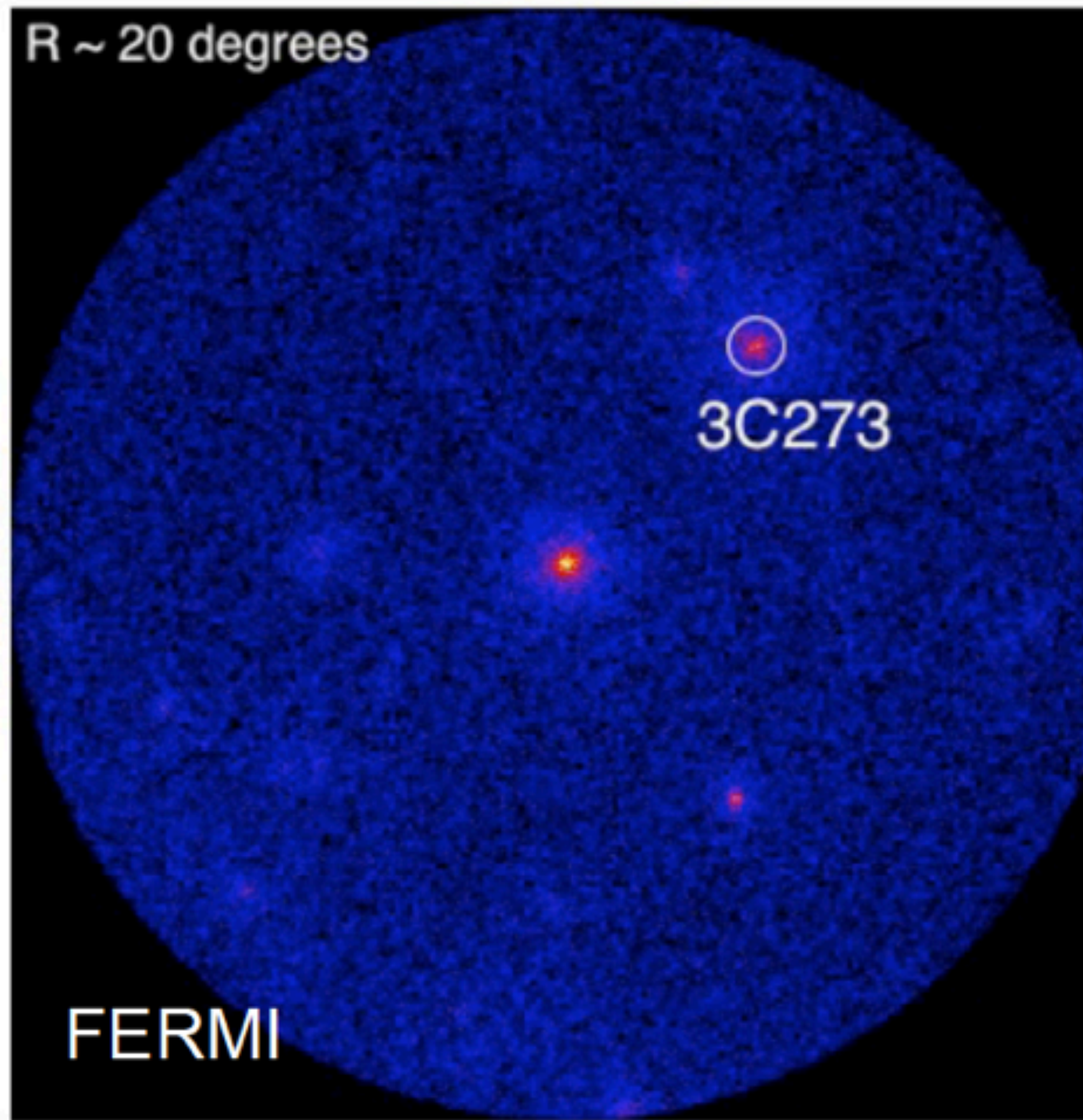


+Z axis of the spacecraft - the line normal to the top surface of the LAT



to avoid gamma-ray photons produced by cosmic ray interacting with the Earth atmosphere

IMAGE

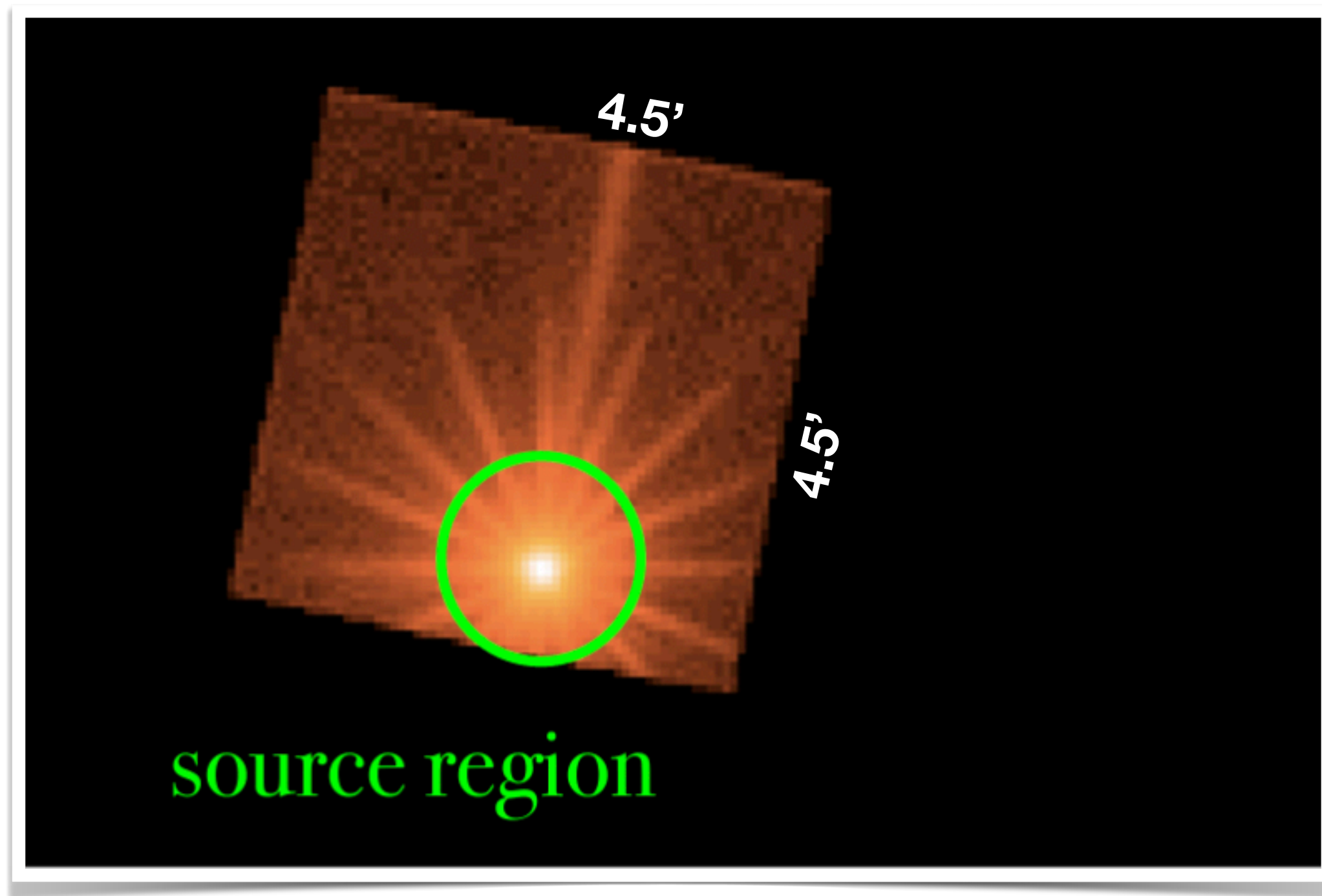


Count map is a 2D representation of the studied region. The events are binned into user-specified rectangular pixels

A 3-D data cube (spatial +energy) is a 'set' of count maps produced at different energy bins.

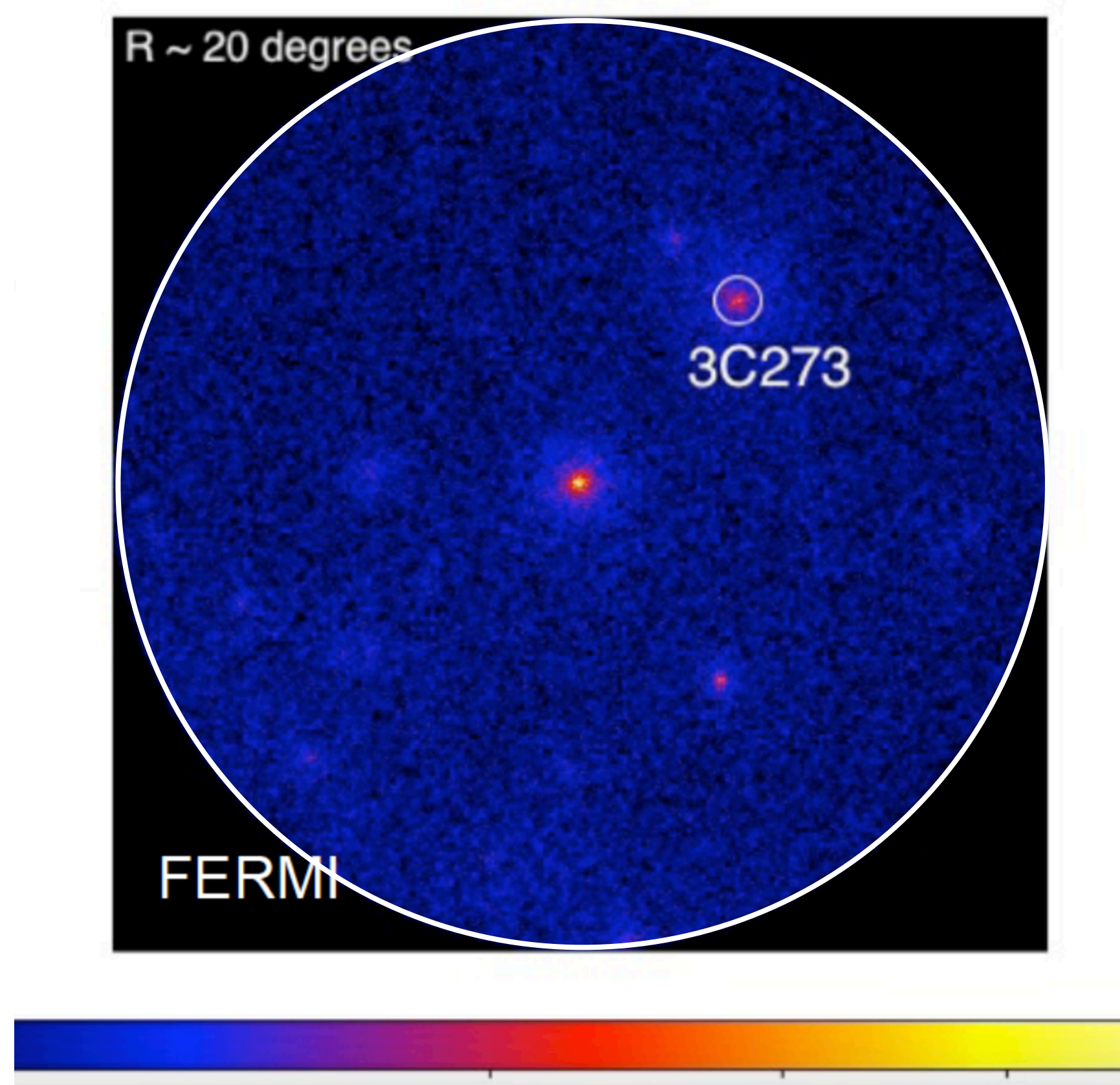
X-rays

Region (") of the source (generally circular)



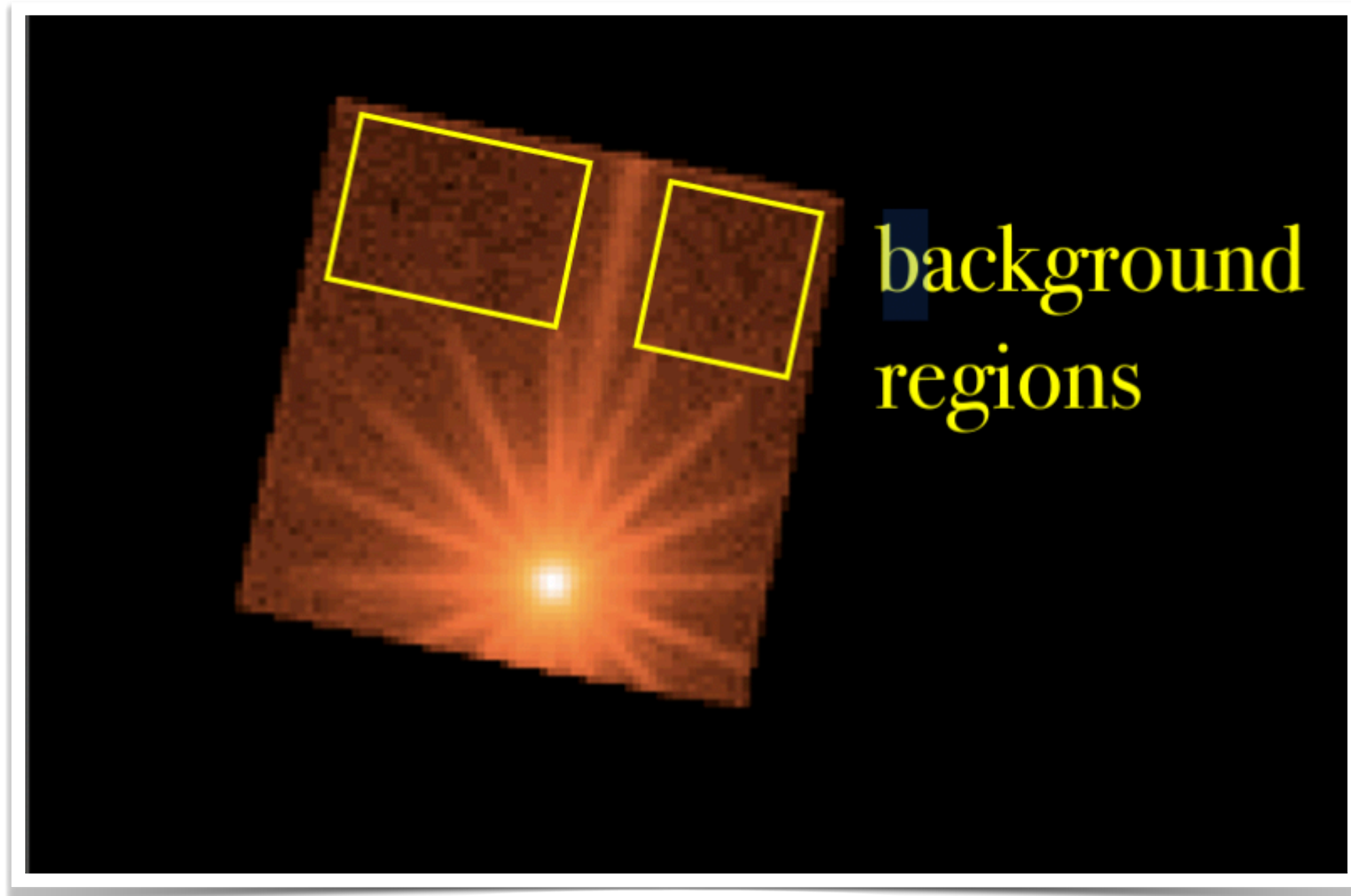
Gamma-rays : FERMI

Region of interest (ROI) of several degrees, including all the sources in the target environment, and the background

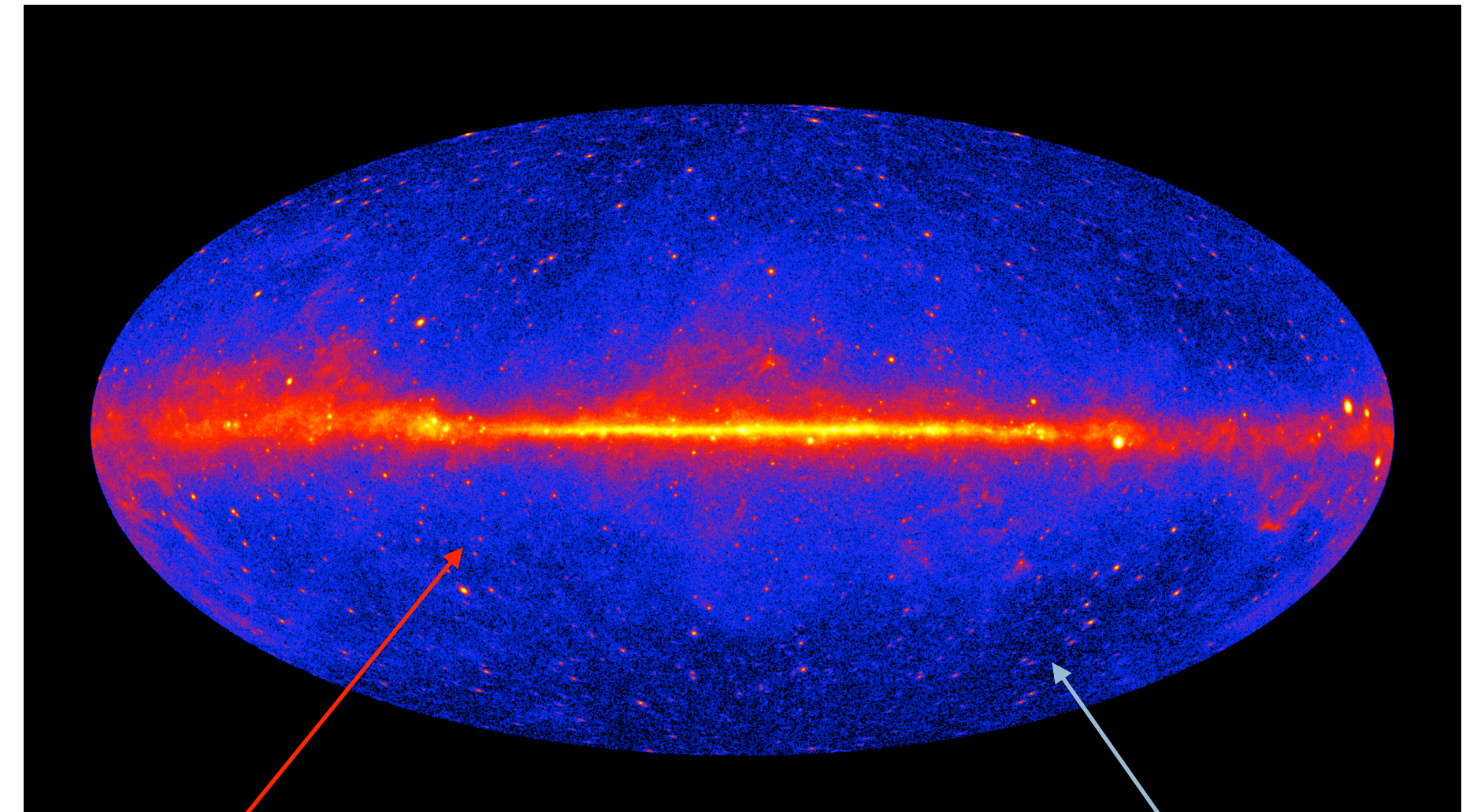


X-rays

Background region (") near the source



Gamma-rays : FERMI



Galactic Gamma-ray background

dominated by emission from interstellar processes in the Milky Way due to energetic particle interactions in the ISM, primarily protons and electrons

Isotropic Gamma-ray background

dominated by superposition of all unresolved extragalactic sources

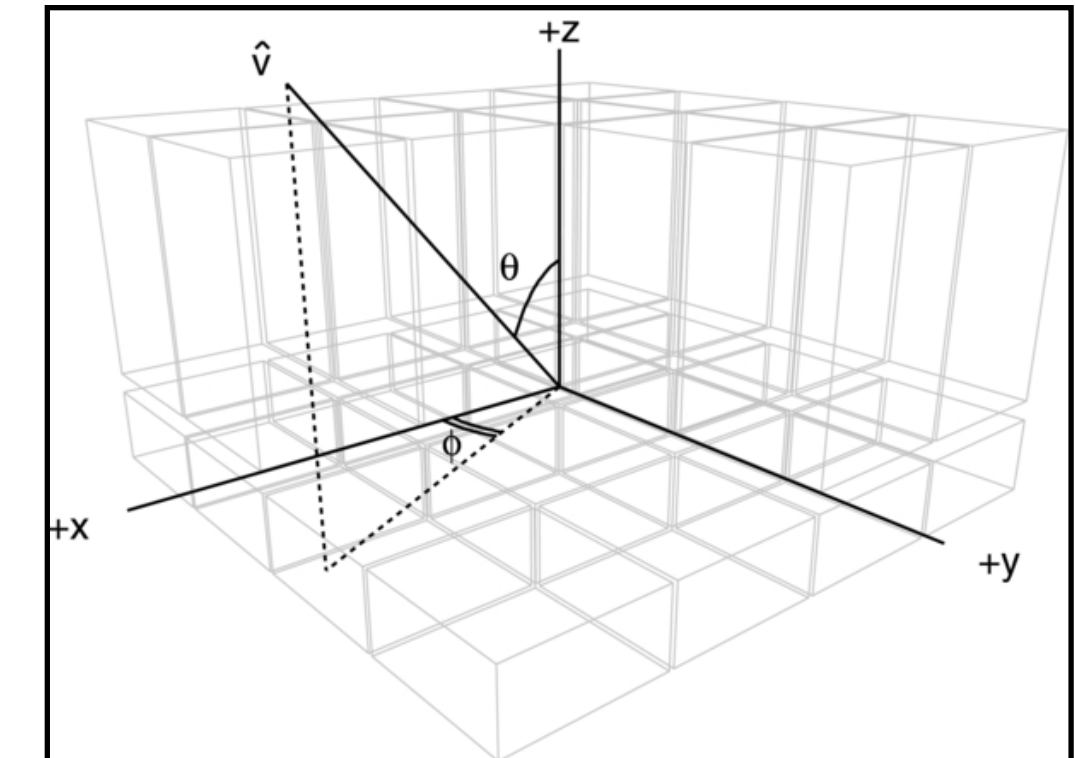
Ancillary file (.arf)

Response matrix (.rmf)

Instrument Response Function IRF

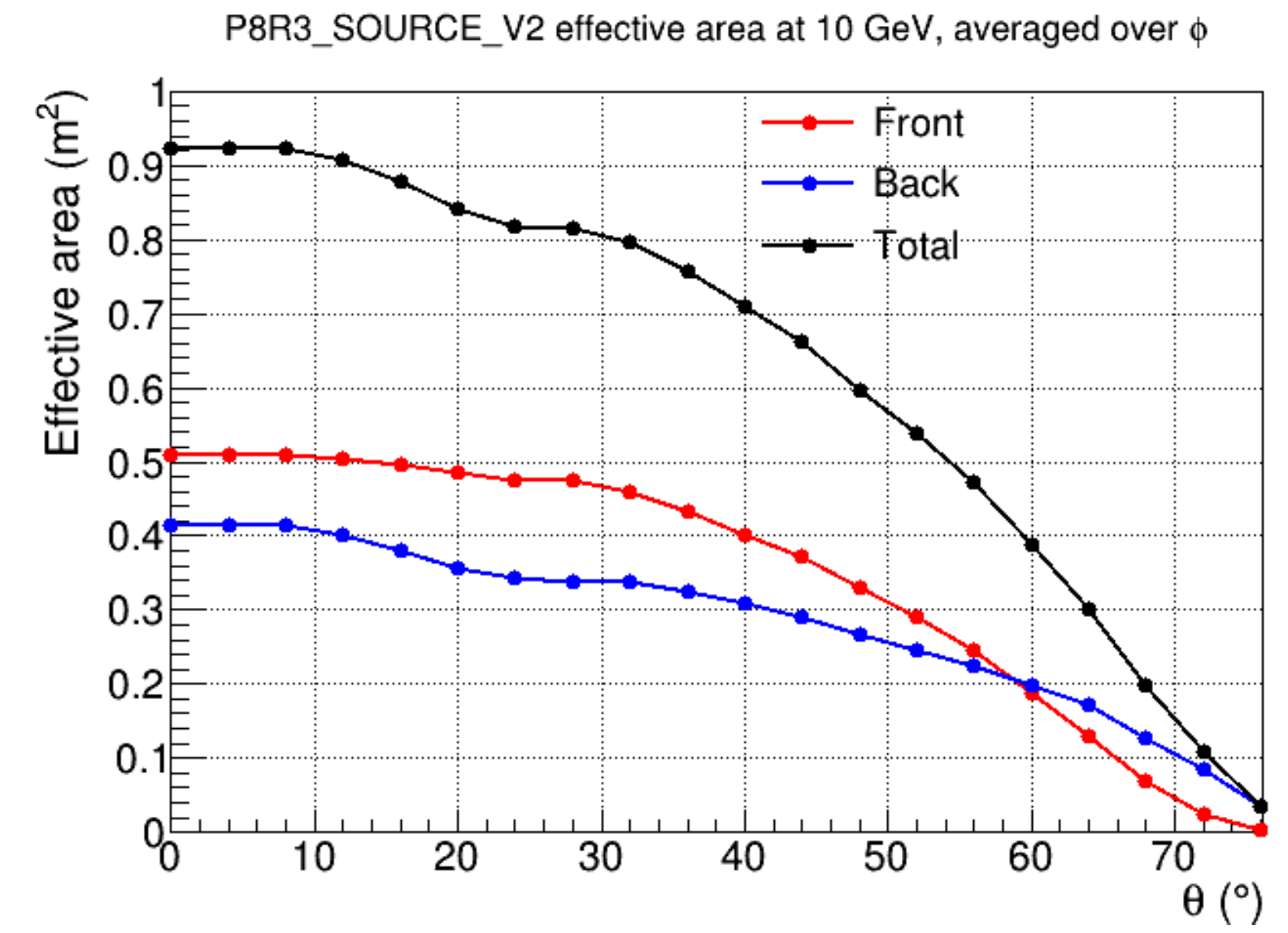
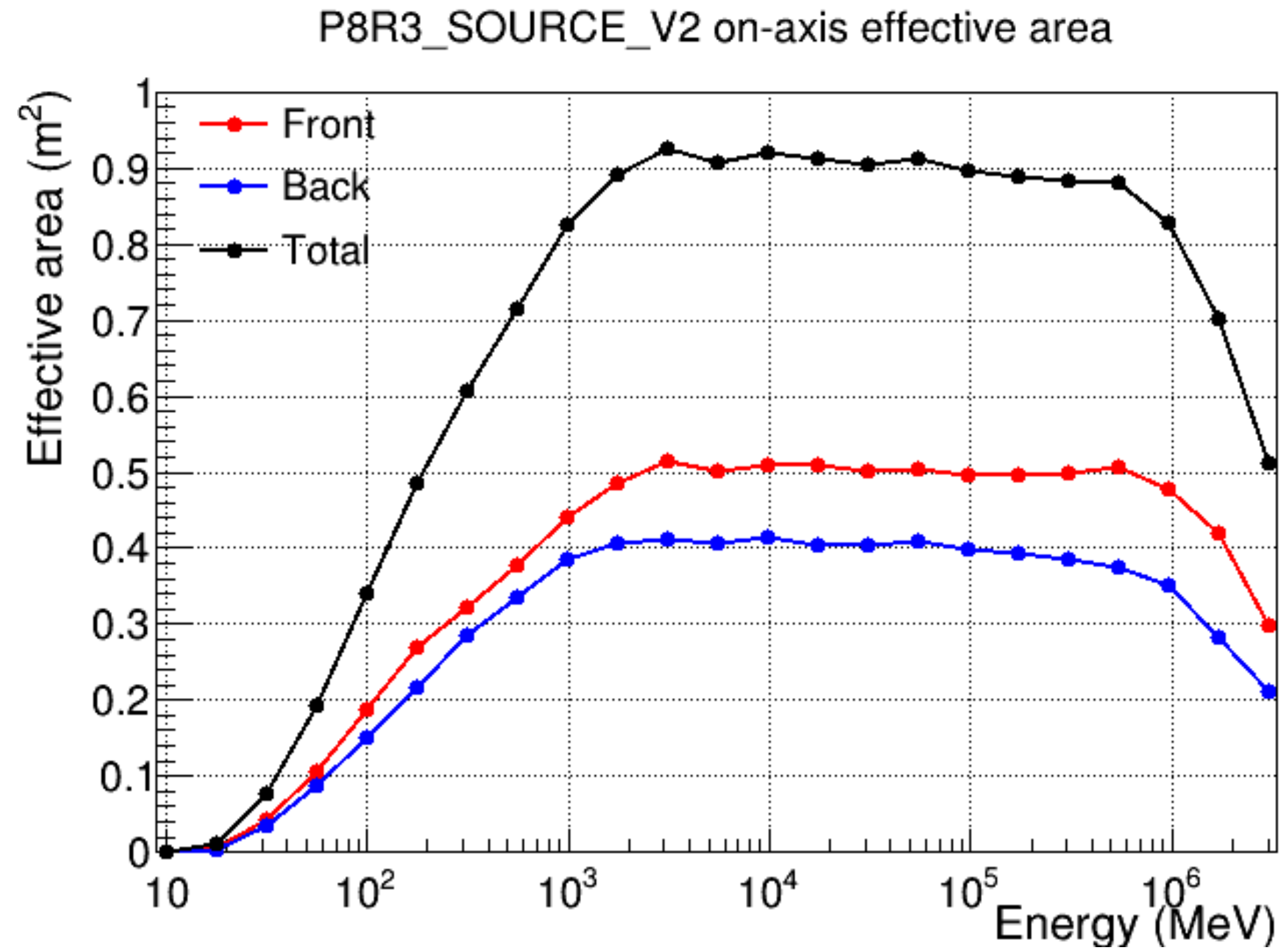
Each event class and event type selection (s) has its own IRFs

$$\mathbf{R} = \mathbf{A}_{\text{eff}} * \mathbf{PSF} * \mathbf{D}$$

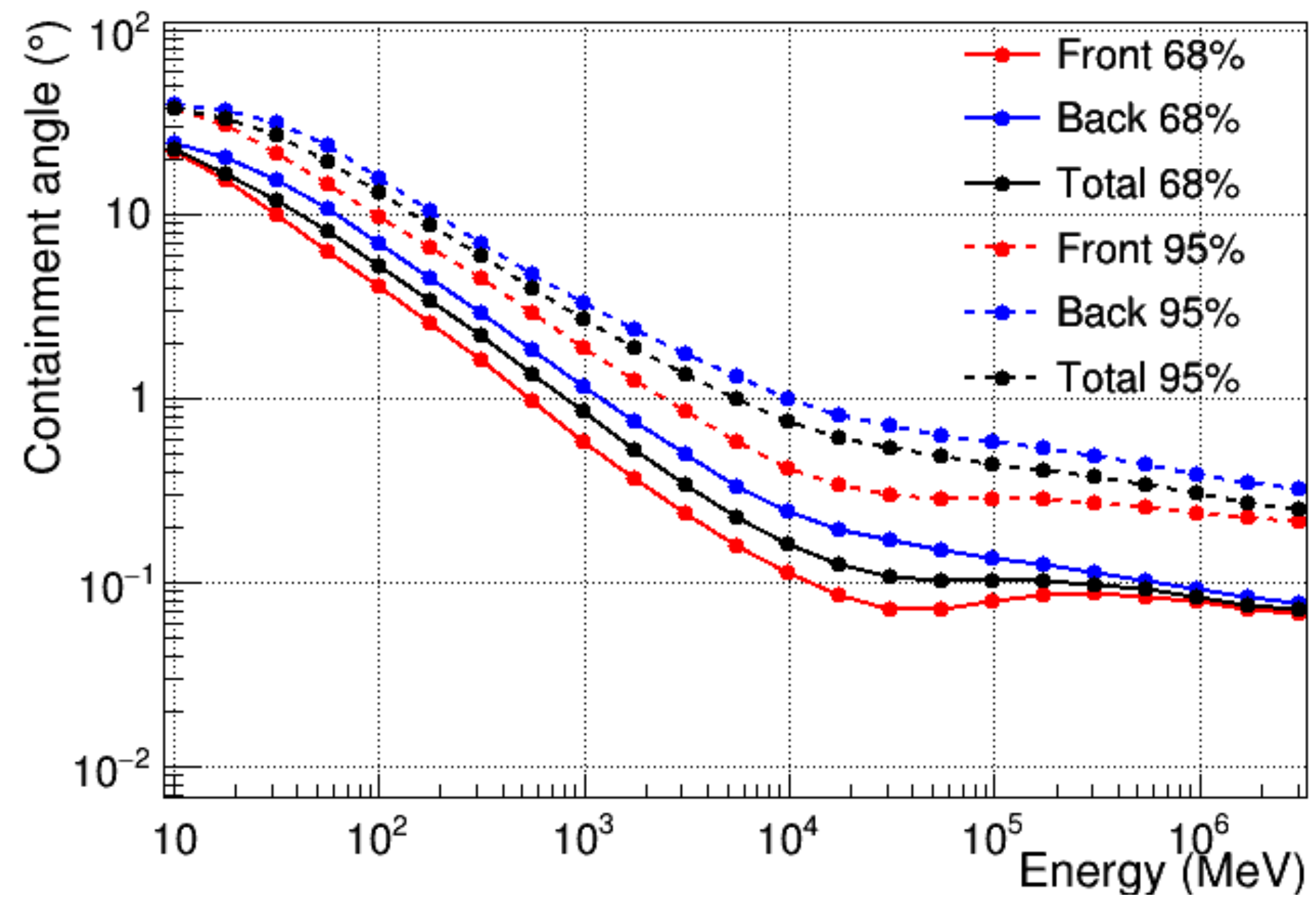


1. *Effective area*, $A_{\text{eff}}(E, \hat{v}, s)$, the product of the cross-sectional geometrical collection area, γ -ray conversion probability, and the efficiency of a given event selection (denoted by s) for a γ ray with energy E and direction \hat{v} in the LAT frame.
2. *Point-spread function (PSF)*, $P(\hat{v}'; E, \hat{v}, s)$, the probability density to reconstruct an incident direction \hat{v}' for a γ ray with (E, \hat{v}) in the event selection s .
3. *Energy dispersion*, $D(E'; E, \hat{v}, s)$, the probability density to measure an event energy E' for a γ ray with (E, \hat{v}) in the event selection s .

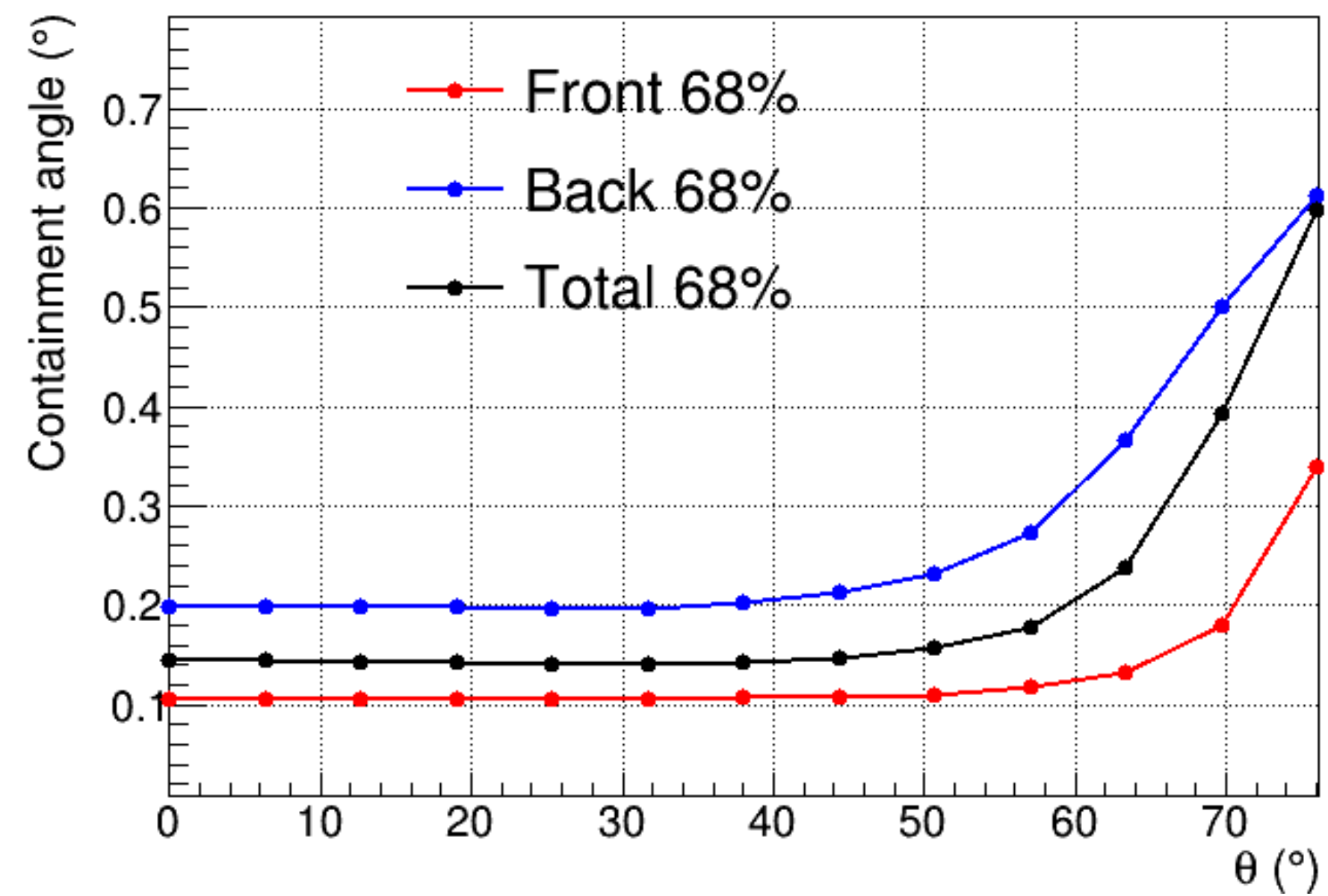
EFFECTIVE AREA



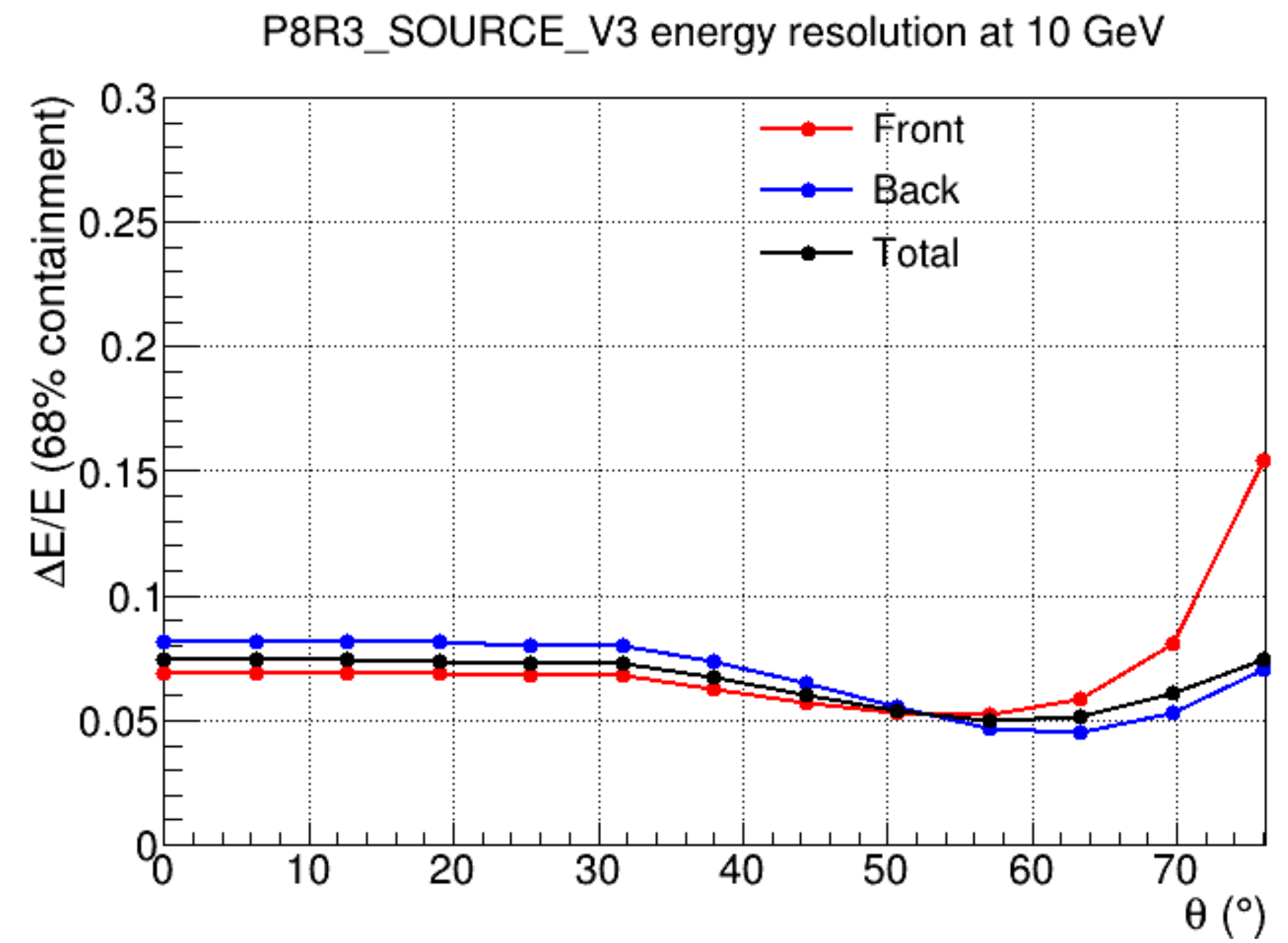
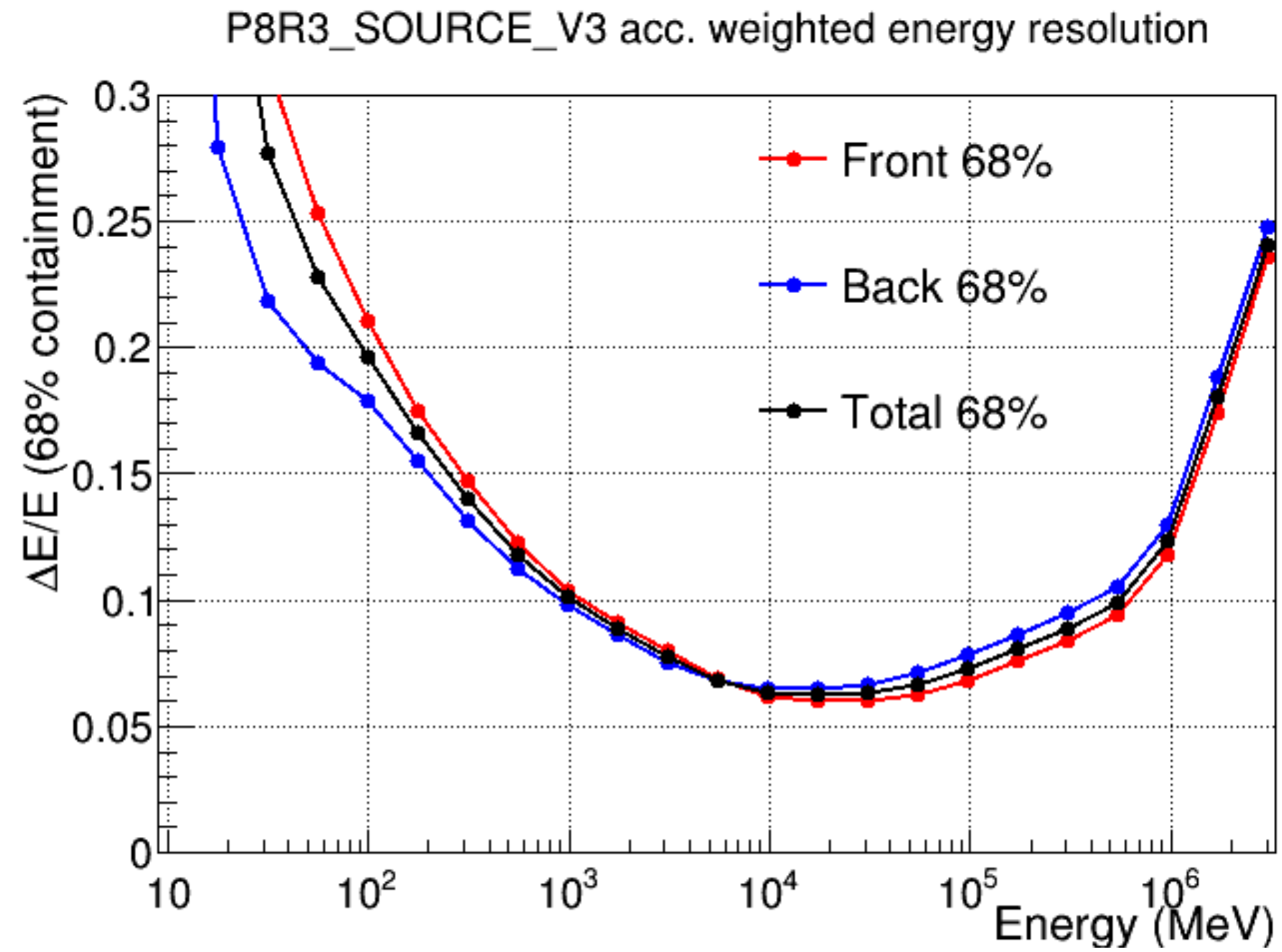
P8R3_SOURCE_V2 acc. weighted PSF



P8R3_SOURCE_V2 PSF at 10 GeV



Energy Resolution



**BECAUSE OF
THE PAUCITY OF EVENTS,
THE LARGE ERRORS ASSOCIATED WITH DETECTING GAMMA-RAYS
A BRIGHT BACKGROUND**

**ANALYSIS AND INTERPRETATION OF DATA
REQUIRE COMPLEX
STATISTICAL TECHNIQUES**

WE NEED A LIKELIHOOD ANALYSIS

The source model is considered as:

$$S(E, \hat{p}, t) = \sum_i s_i(E, t) \delta(\hat{p} - \hat{p}_i) + S_G(E, \hat{p}) + S_{\text{eg}}(E, \hat{p}) + \sum_l S_l(E, \hat{p}, t),$$

Point Sources Galactic & EG Diffuse Sources Other Sources

This model is folded with the Instrument Response Functions (IRFs) to obtain the predicted counts in the measured quantity space (E', p', t') :

$$M(E', \hat{p}', t) = \int_{\text{SR}} dE d\hat{p} R(E', \hat{p}', t; E, \hat{p}) S(E, \hat{p}, t)$$

where

$$\mathbf{R} = \mathbf{A}_{\text{eff}} * \mathbf{PSF} * \mathbf{D}$$

and the

integral is performed over the Source Region, i.e. the sky region encompassing all sources contributing to the Region-of-Interest (ROI). In the standard analysis, only steady sources are considered

$$S(E, \hat{p}, t) \rightarrow S(E, \hat{p})$$

The number of counts in each bin is small and this is characterized by the Poisson distribution

$$p_{\lambda}(n) = \frac{\lambda^n}{n!} e^{-\lambda}$$

λ AVERAGE NUMBER OF EVENTS

n NUMBER OF EVENTS IN EACH BIN

L IS THE PRODUCT OF THE PROBABILITIES OF OBSERVING n_k COUNTS IN EACH BIN (k) WHEN THE NUMBER OF COUNTS PREDICTED BY THE MODEL IS m_k

$$L = \prod_k \frac{m_k^{n_k} e^{-m_k}}{n_k!} = \prod_k e^{-m_k} \prod_k \frac{m_k^{n_k}}{n_k!} = e^{-N_{pred}} \prod_k \frac{m_k^{n_k}}{n_k!}$$

$$\log L = -N_{Pred} + \sum_K n_k \log(m_k) - \log(n!)$$

natural logarithmic of L

It does not depend on model .
It can be neglected

The Test Statistic is defined as

$$TS = -2 \log \left(\frac{\mathcal{L}_{\max,0}}{\mathcal{L}_{\max,1}} \right)$$

where $\mathcal{L}_{\max,0}$ is the maximum likelihood value for a model without an additional source (the 'null hypothesis') and $\mathcal{L}_{\max,1}$ is the maximum likelihood value for a model with the additional source at a specified location.

In the limit of a large number of counts, Wilk's Theorem states that the TS for the null hypothesis is asymptotically distributed as χ_n^2 where n is the number of parameters characterizing the additional source.

As a basic rule of thumb, the square root of the TS is approximately equal to the detection significance for a given source.



Light curve and variability test

A light curve is produced by dividing the data into time bins and applying the likelihood analysis procedure to each.

To test the variability based on the TSvar index defined as :

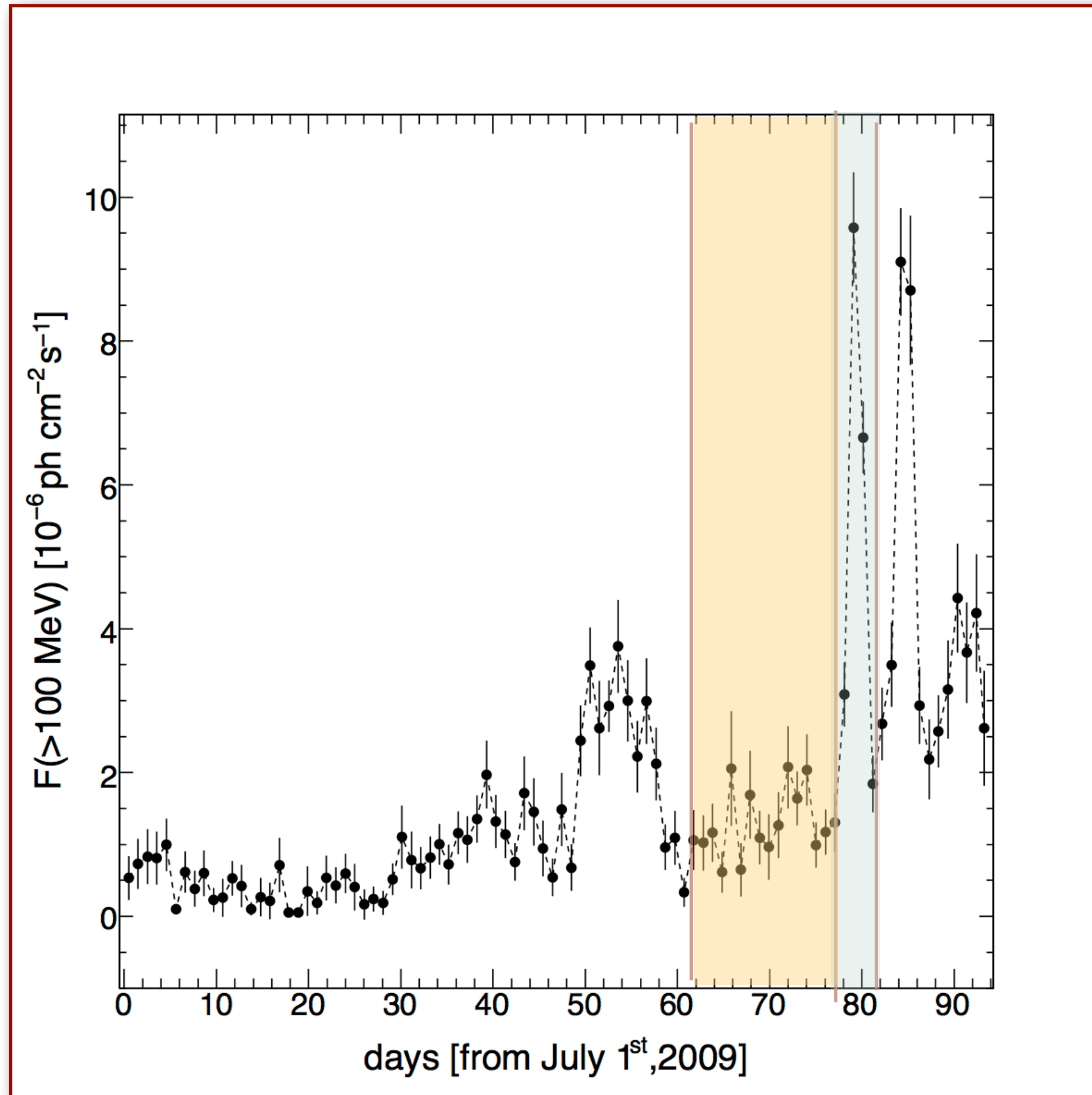
$$TS_{\text{var}} = 2 \sum_i \log \left[\frac{\mathcal{L}_i(F_i)}{\mathcal{L}_i(F_{\text{glob}})} \right]$$

$\mathcal{L}_i(F_{\text{glob}})$ is the likelihood obtained in the fit over the total time

$\mathcal{L}_i(F_i)$ is the likelihood obtained in each interval by freezing the spectral parameters and adjusting the normalization

TS_{var} is distributed as χ^2 with n-1 degree of freedom , where n is the number of time bins.

Light Curve



Spectra

$$F(> 100 \text{ MeV}) = \int_{100}^{\infty} k \left(\frac{E}{E_0}\right)^{-\Gamma} dE$$

